The EMBO Journal Vol.18 No.1 pp.131–144, 1999

Ca^{2+} permeation in cyclic nucleotide-gated channels

Claudia Dzeja, Volker Hagen[1], U.Benjamin Kaupp[2] and Stephan Frings

Institut für Biologische Informationsverarbeitung, Forschungszentrum Jülich, 52425 Jülich, and [1]Forschungsinstitut für Molekulare Pharmakologie, Alfred-Kowalke-Str. 4, 10315 Berlin, Germany

[2]Corresponding author
e-mail: a.eckert@fz-juelich.de

Cyclic nucleotide-gated (CNG) channels conduct Na^+, K^+ and Ca^{2+} currents under the control of cGMP and cAMP. Activation of CNG channels leads to depolarization of the membrane voltage and to a concomitant increase of the cytosolic Ca^{2+} concentration. Several polypeptides were identified that constitute principal and modulatory subunits of CNG channels in both neurons and non-excitable cells, co-assembling to form a variety of heteromeric proteins with distinct biophysical properties. Since the contribution of each channel type to Ca^{2+} signaling depends on its specific Ca^{2+} conductance, it is necessary to analyze Ca^{2+} permeation for each individual channel type. We have analyzed Ca^{2+} permeation in all principal subunits of vertebrates and for a principal subunit from *Drosophila melanogaster*. We measured the fractional Ca^{2+} current over the physiological range of Ca^{2+} concentrations and found that Ca^{2+} permeation is determined by subunit composition and modulated by membrane voltage and extracellular pH. Ca^{2+} permeation is controlled by the Ca^{2+}-binding affinity of the intrapore cation-binding site, which varies profoundly between members of the CNG channel family, and gives rise to a surprising diversity in the ability to generate Ca^{2+} signals.

Keywords: calcium permeation/cyclic nucleotide/ion channel/olfactory sensory neuron/signal transduction

Introduction

Cyclic nucleotide-gated (CNG) channels of vertebrates are cation channels controlled by the cytosolic concentration of cGMP or cAMP (for recent reviews, see Kaupp, 1995; Biel *et al*., 1996a; Finn *et al*., 1996; Zagotta and Siegelbaum, 1996; Li *et al*., 1997). The channels conduct mixed cation currents, carried by Na^+, K^+ and Ca^{2+} ions, and serve to couple both electrical excitation and Ca^{2+} signaling to changes in cyclic nucleotide concentrations. In vertebrate photoreceptors and olfactory sensory neurons (OSNs), where the role of CNG channels in signal transduction is best understood, CNG channels depolarize the membrane voltage and, in addition, determine the activity of a number of Ca^{2+}-regulated proteins involved in cell excitation and adaptation (reviewed in Kaupp and Koch, 1992; Koch, 1995; Korenbrot, 1995; Frings, 1997). Studies of signal transduction in sensory cells have borne out the central aspect of Ca^{2+} permeation in CNG channel function, and recent discoveries of CNG channels in other cell types, including various populations of brain neurons, stimulated a widespread interest in their permeation properties related to the physiology of non-sensory neurons and non-excitable cells. CNG channels have been proposed to control sperm motility (Weyand *et al*., 1994; Wiesner *et al*., 1998), axon guidance (Coburn and Bargmann, 1996) as well as synaptic transmission (Rieke and Schwartz, 1994; Savchenko *et al*., 1997) and plasticity (Zufall *et al*., 1997). Ca^{2+} entry through CNG channels is of particular interest in this context because it represents an alternative pathway for Ca^{2+} entry that is virtually independent of membrane voltage, and links cAMP/cGMP signaling and Ca^{2+} homeostasis without utilizing protein kinases.

A number of biophysical studies have revealed that striking differences in the interaction with Ca^{2+} ions distinguish CNG channels in rod and cone photoreceptors and OSNs (Nakatani and Yau, 1988; Colamartino *et al*., 1991; Perry and McNaughton, 1991; Root and MacKinnon, 1993; Zufall and Firestein, 1993; Eismann *et al*, 1994; Frings *et al*., 1995; Park and MacKinnon, 1995; Picones and Korenbrot, 1995). Ca^{2+} ions enter the channel from the external solution and bind to a set of glutamate residues within the channel pore (Root and MacKinnon, 1993; Eismann *et al*., 1994; Park and MacKinnon, 1995). In the accompanying paper (Seifert *et al*., 1999), we show that these glutamate residues form binding sites of distinctively different Ca^{2+} affinity, which is expected to cause a pronounced diversity in Ca^{2+} permeation. Here we analyze the relationship between Ca^{2+} affinity and Ca^{2+} permeation quantitatively. We examine four CNG channel types whose Ca^{2+} affinity was determined previously by Ca^{2+} blockage (Baumann *et al*., 1994; Frings *et al*., 1995), and study Ca^{2+} permeation by measuring the fractional Ca^{2+} current at physiological ion concentrations. We manipulate Ca^{2+} affinity experimentally by changing membrane voltage and extracellular pH and explore the consequences for Ca^{2+} permeation. Furthermore, we investigate the influence of modulatory channel subunits that co-assemble with the principal subunits and alter the structure of the intrapore binding site. Of particular interest are modulatory subunits that contribute to the binding site uncharged glycine residues and have been shown to reduce Ca^{2+} affinity (Körschen *et al*., 1995). The results of these studies provide a framework for understanding the molecular basis of Ca^{2+} permeation in CNG channels. They show that the amount of Ca^{2+} entering a cell through these channels is determined by the binding affinity of the intrapore binding site, and that Ca^{2+} permeation critically depends on the set of CNG channel subunits expressed by a cell.

Results

We measured the contribution of Ca^{2+} current, I_{Ca}, to the total channel current, I_T, passing through heterologously expressed CNG channels under physiological conditions. We combined whole-cell recordings of I_T with measurements of the Ca^{2+}-induced changes in fluorescence intensity from FURA-2-loaded cells (F_{380}) to determine the ratio of Ca^{2+} current to total current (I_{Ca}/I_T), called fractional Ca^{2+} current or P_f (Neher and Augustine, 1992; Schneggenburger *et al*., 1993; Frings *et al*., 1995)

$$P_f = \frac{I_{Ca}}{I_T} \quad (1)$$

Several conditions must be fulfilled to obtain a reliable measure of P_f. (i) The Ca^{2+}-buffering capacity of FURA-2 must greatly exceed the endogeneous Ca^{2+}-buffering capacity of the cell. (ii) The Ca^{2+}-induced fluorescence decrement (ΔF_{380}) and the time integral of the cGMP-induced current $\int I_T dt$ (i.e. the amount of charge transported by CNG channels) must be strictly proportional to each other. (iii) The relationship between Ca^{2+} entry and the change in F_{380} must be known. Experiments performed to fulfill these conditions are described in Materials and methods. An important prerequisite for accurate determination of P_f is the fast and controlled activation of CNG channels. In an initial approach to measure P_f in CNG channels, we loaded cells with 8-Br-cGMP while blocking the channels with extracellular Mg^{2+} (Frings *et al*., 1995). Removal of Mg^{2+} opened the channels, and I_T and F_{380} were recorded. However, this method had severe limitations and allowed P_f recordings at physiological levels of extracellular Ca^{2+}, $[Ca^{2+}]_o$, only in one CNG channel type. The relatively slow decline of Mg^{2+} blockage during washout hampered analysis of small signals. In addition, Mg^{2+} is not a perfect blocker for CNG channels, and competition of Ca^{2+} with Mg^{2+} for the cation-binding site resulted (particularly at higher levels of $[Ca^{2+}]_o$) in substantial Ca^{2+} influx even before Mg^{2+} washout. To overcome these technical limitations, we used a different strategy for channel activation for the present study (Figure 1A). Cells were filled with caged cGMP or caged 8-Br-cGMP, which are photolabile, biologically inactive derivatives of channel ligands (Corrie and Trentham, 1993; Hagen *et al*., 1996, 1998). These substances release ligand upon irradiation with a flash of UV light, inducing channel activation within a few milliseconds (Karpen *et al*., 1988; Hagen *et al*., 1996). The amount of ligand liberated by a single flash is limited by two factors: the solubility of the caged compounds in physiological solutions does not exceed 120–150 μM (Hagen *et al*., 1996, 1998); and the duration and intensity of the light flash must be limited to prevent bleaching of FURA-2 which would bias P_f measurements. Due to these limitations, only 10–20 μM of ligand could be photoreleased by a single flash, which was, however, sufficient to obtain P_f measurements from all channel types investigated. Figure 1B shows an example of such an experiment. The light flash (arrow) induces an inward current (I_T) that declines after reaching a maximum due to degradation of photoreleased cGMP by endogeneous phosphodiesterase activity. Together with I_T, a change in the fluorescence signal ($-F_{380}$) is recorded that originates from Ca^{2+} influx and binding of Ca^{2+} ions to the dye. The fractional Ca^{2+} current is calculated from the two signals as described in Materials and methods. Using this method, we were able to obtain P_f values over the whole range of $[Ca^{2+}]_o$ for all channel types.

With its wide range of Ca^{2+} affinities, the CNG channel family offers a unique opportunity to address the following questions. (i) To what extent does the fractional Ca^{2+} current differ between CNG channels of different Ca^{2+} affinity? (ii) How does P_f depend on the extracellular Ca^{2+} concentration? (iii) How sensitively does P_f respond to modifications of Ca^{2+} affinity by changes in V_m or extracellular pH? (iv) What is the influence of modulatory channel subunits on P_f?

CNG channels show large differences in Ca^{2+} permeation

The CNG channel family of vertebrate ion channels is encoded by five distinct genes that generate three principal and two modulatory subunits. The principal subunits CNCα1 (first identified in rod photoreceptors; Kaupp *et al*., 1989), CNCα2 (first identified in cone photoreceptors; Bönigk *et al*., 1993; Weyand *et al*., 1994) and CNCα3 (first identified in OSNs; Dhallan *et al*., 1990; Ludwig *et al*., 1990) form functional CNG channels when heterologously expressed as homomeric proteins. Modulatory subunits do not express functional CNG channels by themselves, but they co-assemble with principal subunits and determine important channel properties including ligand sensitivity and ion selectivity. The modulatory subunit CNCα4 was identified in rat OSNs (Bradley *et al*., 1994; Liman and Buck, 1994) and was shown recently to be associated with the native olfactory channel (Sautter *et al*., 1998). Additional modulatory subunits are derived by alternative exon usage from a fifth gene, CNCβ1, and were shown to co-assemble with CNCα1 in the native transduction channels of rod photoreceptors (CNCβ1a; Chen *et al*., 1994; Körschen *et al*., 1995) and with CNCα3 in OSNs (CNCβ1b; Sautter *et al*., 1998). In this study, we use the following abbreviations for simplicity: bR for homomeric bovine CNCα1 channels, bC for bovine CNCα2 and bO for bovine CNCα3. In addition, we investigate a CNG channel cloned from *Drosophila melanogaster* sensory organs (Baumann *et al*., 1994; here referred to as Dm).

Figure 2A shows recordings of I_T and F_{380} from one cell expressing bC at 0.1 mM $[Ca^{2+}]_o$ and from another cell at 1 mM $[Ca^{2+}]_o$. I_T is 10 times larger at 0.1 mM (left traces) than at 1 mM (right traces), whereas the fluorescence signals, i.e. the Ca^{2+} influx, are largely similar (compare traces in Figure 2A). Accordingly, P_f values determined from these cells were 0.023 and 0.33 at the low and high $[Ca^{2+}]_o$, respectively, demonstrating that elevated levels of $[Ca^{2+}]_o$ strongly increase the fractional Ca^{2+} current. We determined the dependence of P_f on $[Ca^{2+}]_o$ for each type of CNG channel by varying $[Ca^{2+}]_o$ over the entire range of physiological concentrations, while keeping the concentrations of other permeable cations constant. The Ca^{2+} dependence of P_f is illustrated in Figure 2B, which presents collected results from 61 cells expressing bC. P_f increases steeply between 0.3 and 3 mM Ca^{2+} and reaches unity at $[Ca^{2+}]_o \geqslant 6$ mM, indicating that bC conducts a pure Ca^{2+} current at this concentration. The Ca^{2+} dependence of P_f is characterized

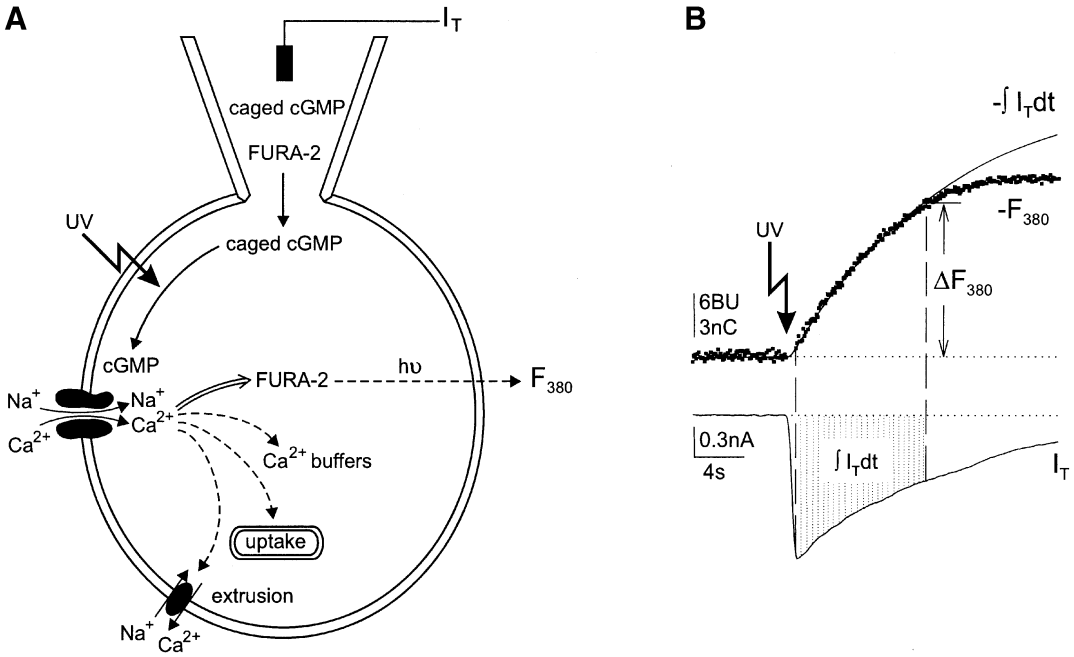

Fig. 1. Determination of the fractional Ca^{2+} current in CNG channels. (**A**) Experimental design: an HEK-293 cell expressing CNG channels is loaded through a patch pipette in the whole-cell configuration with caged cGMP and FURA-2. Photorelease of cGMP by a UV flash leads to activation of channels that conduct both Na^+ and Ca^{2+}. An electrode inside the patch pipette records the total current, I_T, and Ca^{2+} entry is monitored by changes in the FURA-2 fluorescence, F_{380}, recorded by a photon counter. For quantitative recording of Ca^{2+} influx, FURA-2 is used at a concentration of 1–2 mM, which prevents loss of inflowing Ca^{2+} to cellular Ca^{2+} buffers and transport systems. (**B**) Evaluation of data recorded at –70 mV from a cell expressing bO. $[Ca^{2+}]_o$ was 0.3 mM; the pipette contained 75 μM caged cGMP and 1 mM FURA-2. The experiment was started with a 500 ms UV flash of 0.6 mW (arrow). Whole-cell current (I_T) and FURA-2 fluorescence ($-F_{380}$) were recorded simultaneously. Fluorescence intensity is given in bead units (BU). Superposition of fluorescence and current integral ($-\int I_T dt$, given in nanoCoulomb) indicates proportionality within the time segment marked by the vertical lines. This segment is used to calculate the value of $f = \Delta F_{380}/\int I_T dt$, and to determine the fractional Ca^{2+} current, P_f, as described in Materials and methods.

by the P_f constant, K_{Pf}, representing the value of $[Ca^{2+}]_o$ at which half of the current is carried by Ca^{2+} ($P_f = 0.5$). K_{Pf} has a characteristic value for each CNG channel type and was found to be 1.38 mM for bC.

P_f values were obtained from cells expressing channels at different densities. This raises the concern that local changes of ion concentrations may occur at high current densities, as reported previously for photoreceptors (Zimmerman *et al*., 1988). Because of the steep Ca^{2+} dependence of P_f, a drop in the local Ca^{2+} concentration at the extracellular channel entry may relieve Ca^{2+} blockage and reduce Ca^{2+} permeation. To investigate whether such a local Ca^{2+} depletion has biased the P_f data, we studied the relationship between P_f values and current density. As a measure of current density, the total current at 0.3 mM Ca^{2+} was related to the membrane capacitance (which is proportional to the cell surface area). A plot of P_f against the current density (inset in Figure 2B) shows no systematic change of P_f over a 30-fold range of current density (1.5–50.8 pA/pF). This result shows that P_f values are not diminished through local depletion of extracellular Ca^{2+} under our experimental conditions.

Analyzing the Ca^{2+} dependence of P_f for bR was more demanding because bR is extremely sensitive to blockage by extracellular Ca^{2+} (Root and MacKinnon, 1993; Eismann *et al*., 1994; Frings *et al*., 1995). Currents and fluorescence signals recorded in the presence of Ca^{2+} from cells expressing bR were much smaller than with other channels. Channel densities, however, were similar, since bR-, bC- and bO-expressing cells produced up to 1 nA of Na^+ current in Ca^{2+}-free solution at –70 mV. Using caged compounds, it was possible to obtain P_f measurements at four different Ca^{2+} concentrations and to determine K_{Pf}. Cells expressing a high density of bR channels could be analyzed when caged 8-Br-cGMP was used for channel activation, because bR channels display higher sensitivity for 8-Br-cGMP ($K_{1/2}$ = 9.5 μM) than for cGMP ($K_{1/2}$ = 80 μM; Altenhofen *et al*., 1991). Nevertheless, full activation of channels was not accomplished because the photorelease of 8-Br-cGMP was limited by solubility of the caged compound and light intensity as discussed above. Control experiments without caged 8-Br-cGMP ensured that neither current nor fluorescence recordings were altered by effects unrelated to channel activation (Figure 2C). The Ca^{2+} dependence of P_f is characterized by a K_{Pf} of 0.41 mM (Figure 2D; 17 cells), demonstrating that bR conducts a pure Ca^{2+} current already at 1 mM $[Ca^{2+}]_o$. This result is at variance with a P_f value that we obtained in a previous attempt to measure fractional Ca^{2+} currents in bR channels using the Mg^{2+} washout technique (Frings *et al*., 1995). We measured a much lower value for P_f at 0.3 mM $[Ca^{2+}]_o$ as a result of inaccuracy in the determination of I_T and F_{380} during Mg^{2+} washout. Particularly when analyzing very small signals in a P_f experiment, rapid channel activation is a critical pre-condition for obtaining reliable measurements, and this cannot be achieved by the relatively slow Mg^{2+} washout technique.

Ca^{2+} blockage of bO is comparable with bC (K_i = 92 μM at –70 mV; Frings *et al*., 1995) so that signals of similar size were recorded even at millimolar $[Ca^{2+}]_o$.

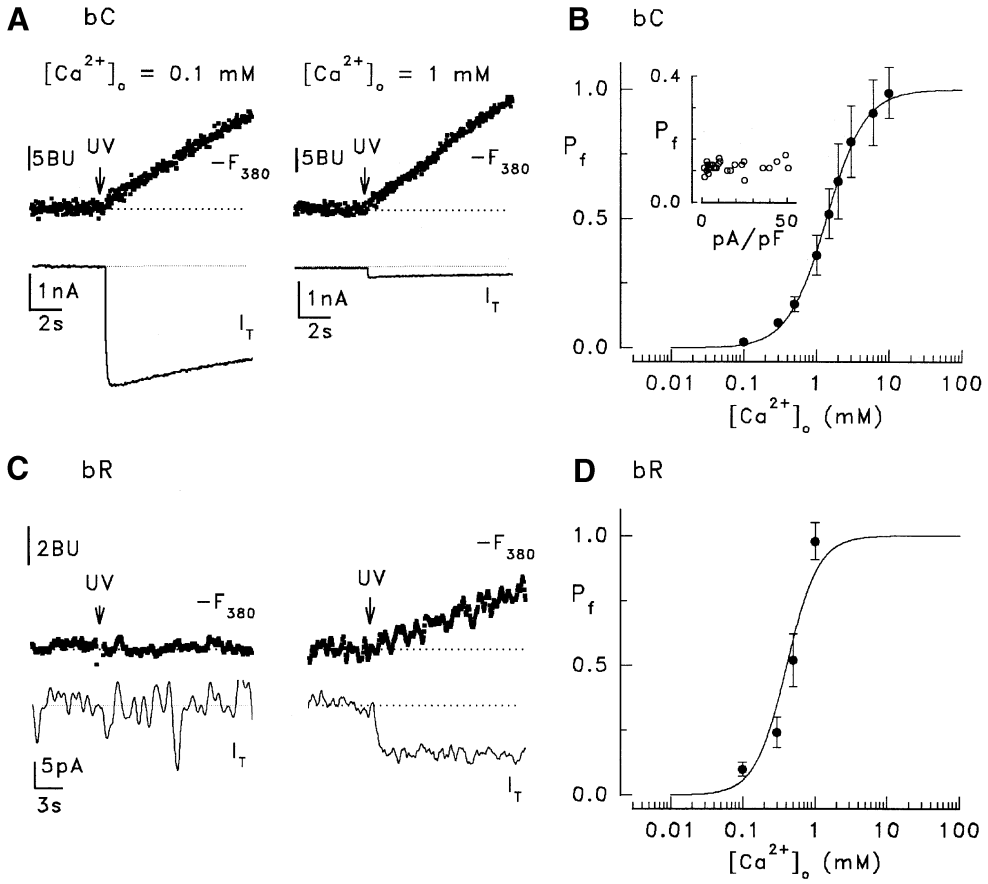

Fig. 2. The fractional Ca^{2+} current of bC and bR channels. (**A**) The relationship of current, I_T and fluorescence, $-F_{380}$, in bC at the indicated concentrations of extracellular Ca^{2+}, $[Ca^{2+}]_o$. Recordings from two different cells at –70 mV with 150 µM caged cGMP and 2 mM FURA-2. Flash duration: 20 ms. The slow decay of inward currents results from hydrolysis of cGMP by endogenous phosphodiesterase activity (for details, see Hagen *et al*., 1996). This decay is irrelevant to the P_f measurements as it only reflects a decrease in P_o (see below). (**B**) Dependence of P_f on $[Ca^{2+}]_o$ for bC at –70 mV. To determine the value of $[Ca^{2+}]_o$ where half of the channel current is carried by Ca^{2+} (the P_f constant K_{Pf}), the solid line was constructed using a Hill-type equation ($P_f = c^n/[c^n + (K_{Pf})^n]$, $c = [Ca^{2+}]_o$) with K_{Pf} = 1.38 mM. Inset: plot of P_f against current density. The maximal flash-induced current in each cell is related to the membrane capacitance. P_f data were obtained from 27 cells at 0.3 mM $[Ca^{2+}]_o$ and –70 mV, and show no systematic variation with current density. (**C**) Simultaneous current and fluorescence recordings from two cells expressing bR without (left panel) and with (right panel) caged 8-Br-cGMP in the pipette solution. The flash duration was 100 ms (arrows), with V_m = –70 mV, $[Ca^{2+}]_o$ = 1 mM, 2 mM FURA-2 and 120 µM caged 8Br-cGMP. The control experiment on the left shows that the UV flash does not induce current or fluorescence signals unrelated to CNG channels. (**D**) Ca^{2+} dependence of P_f for bR at –70 mV. The solid line was constructed with K_{Pf} = 0.41 mM.

Table I. Fractional Ca^{2+} current P_f of four homomeric CNG channels

$[Ca^{2+}]_o$ (mM)	bC	bR	bO	Dm
0.1	0.02±0.01 (5)	0.10±0.03 (4)	0.05±0.02 (7)	0.01±0.01 (5)
0.3	0.10±0.01 (4)	0.24±0.06 (4)	0.13±0.02 (9)	0.03±0.016 (7)
0.5	0.17±0.03 (9)	0.52±0.10 (6)	0.21±0.04 (8)	0.05±0.01 (12)
1	0.36±0.08 (10)	0.98±0.07 (3)	0.39±0.07 (8)	0.10±0.02 (9)
1.5	0.52±0.10 (5)	–	0.55±0.08 (5)	–
2	0.65±0.14 (8)	–	0.67±0.12 (6)	0.22±0.04 (4)
3	0.80±0.14 (11)	–	0.85±0.13 (5)	0.35±0.05 (5)
6	0.91±0.13 (6)	–	0.95±0.13 (3)	0.66±0.10 (5)
10	0.99±0.10 (3)	–	1.01±0.12 (2)	0.79±0.10 (6)
20	–	–	–	1.03±0.17 (5)
K_{Pf} (mM)	1.38	0.41	1.24	4.16

P_f values were measured at –70 mV. K_{Pf} values indicate the Ca^{2+} concentration for P_f = 0.5.

The collected data for nine different Ca^{2+} concentrations obtained from 53 cells (Figure 3, filled squares) yielded a K_{Pf} of 1.24 mM, which is in good agreement with our previous value (1.1 mM; Frings *et al*., 1995), illustrating that bO resembles bC both in its Ca^{2+} affinity and its ability to conduct pure Ca^{2+} currents at low millimolar $[Ca^{2+}]_o$. The Ca^{2+} dependence of P_f for the *D.melanogaster* CNG channel, Dm, was shifted to much higher levels of $[Ca^{2+}]_o$, and the data from 58 cells yielded a K_{Pf} of 4.16 mM (Figure 3, open squares). Thus, the Dm channel

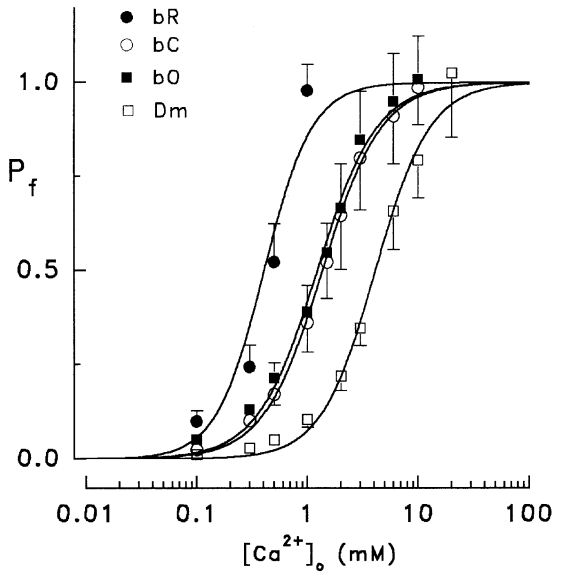

Fig. 3. Dependence of the fractional Ca^{2+} current on $[Ca^{2+}]_o$ for four different CNG channels. Ca^{2+} dependence of P_f is shown for bR (●), bO (■), bC (○) and Dm (□). Solid lines were constructed with K_{Pf} = 1.24 mM for bO and with K_{Pf} = 4.16 mM for Dm. Data for bR and bC are from Figure 2. All P_f values, standard deviations and numbers of experiments are summarized in Table I.

does not conduct a pure Ca^{2+} current at $[Ca^{2+}]_o$ below 10 mM. This is consistent with the observation that Dm shows the lowest Ca^{2+} affinity of the four channel types (K_i = 352 μM at –80 mV; Baumann *et al*., 1994).

All P_f values of the four channel types and the derived constants K_{Pf} are summarized in Table I. Two conclusions can be drawn from these results. First, channels like bR with a high-affinity intrapore Ca^{2+}-binding site are characterized by a low value of K_{Pf}, whereas channels like Dm with a low-affinity Ca^{2+}-binding site display a high value of K_{Pf}. Secondly, all CNG channels can carry a pure Ca^{2+} current in the low millimolar range of $[Ca^{2+}]_o$, even at 10-fold higher concentrations of monovalent cations.

Does P_f depend on the open probability of channels?

Each channel type investigated here has a different ligand sensitivity and, although we used concentrations of caged ligand corresponding to ~10 times the $K_{1/2}$ (see Materials and methods), we could not fully activate CNG channels in our experiments. Because of the limited control of open probability (P_o) in our experiments, our P_f recordings were obtained at different levels of P_o. If the fractional Ca^{2+} current changes with P_o, P_f values obtained at different P_o may not be compared with each other. To test this possibility, we determined P_f values in bO at low and high P_o.

Both measurements were taken from the same cell expressing bO in two successive experiments, taking advantage of the endogeneous phosphodiesterase (PDE) activity that hydrolytically destroys photoreleased cGMP within a few minutes (Hagen *et al*., 1996), allowing repeated P_f measurements with the same cell. First, P_o was adjusted to ~0.1 by using 75 μM caged cGMP and light flashes of 20 ms duration (Figure 4A, left traces; see Materials and methods for estimation of P_o). After

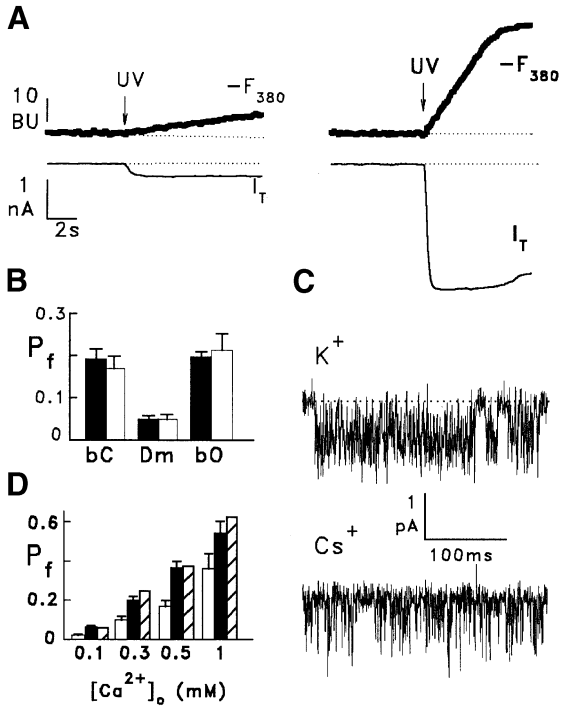

Fig. 4. P_f measurements at low and high open probability. (**A**) Two recordings from the same cell expressing bO with UV flashes of 20 ms (left traces) and 100 ms (right traces) duration. P_o after the first flash was near 0.1. Following hydrolysis of the photoreleased cGMP, the second flash produced a P_o of ~0.9. V_m = –70 mV, $[Ca^{2+}]_o$ = 0.3 mM, 2 mM FURA-2, 75 μM caged 8Br-cGMP. P_f values were 0.11 at low and 0.12 at high P_o. (**B**) Comparison of P_f values measured at 0.5 mM $[Ca^{2+}]_o$ with intracellular K^+ (open bars) or Cs^+ (filled bars) for bC, bO and Dm (V_m = –70 mV). Data are means and standard deviations of 3–12 measurements each. (**C**) Single-channel recording from a bC channel. Inside-out patch with standard extracellular solution (plus 1 mM EGTA) in the pipette, and intracellular solutions containing either K^+ or Cs^+ as main cation and 1 mM cGMP. Recorded at –50 mV, filtered at 1 kHz. The dotted line indicates the closed state of the channel. (**D**) Comparison of P_f values at –70 mV for 0.1, 0.3, 0.5 and 1 mM $[Ca^{2+}]_o$ measured with 120 mM $[Na^+]_o$ (open bars; data from Table I) or 120 mM $[Li^+]_o$ [filled bars; 0.068±0.006 (3); 0.202±0.018 (6); 0.368±0.032 (4); 0.545±0.057 (7)]. The values calculated for $P_f(Li^+)$ using Equation 2 (hatched bars; 0.062, 0.246, 0.376 and 0.623) are consistent with measured values.

recording ΔF_{380} and I_T at low P_o, a period of 3 min was allowed for complete degradation of cGMP by PDE and closure of the channels. A flash of 100 ms was then applied to adjust P_o to ~0.9, and a P_f value at this P_o was obtained from the same cell (Figure 4A, right traces). The mean ratio of P_f values from four such experiments was P_f (low P_o)/P_f (high P_o) = 0.97±0.02, demonstrating that P_f does not depend on P_o under our experimental conditions.

Does the fractional Ca^{2+} current depend on monovalent cations?

In a pioneering work on photoreceptors, Nakatani and Yau (1988) measured the contribution of Ca^{2+} to the dark current conducted by cGMP-gated channels in the plasma membrane of the rod outer segment. The rationale of these experiments utilized the fact that Ca^{2+} enters the photoreceptor through CNG channels and is extruded by a Na^+/Ca^{2+}–K^+ exchanger, which can be inactivated by replacing extracellular Na^+ with Li^+. First, the dark current carried by Li^+ and Ca^{2+} was allowed to enter the

outer segment through CNG channels, and the amount of charges (the current integral) was calculated. Because the exchanger is not active in Li^+ solution, Ca^{2+} was not extruded and accumulated within the cell. To count the accumulated Ca^{2+} ions, CNG channels were closed by illumination of the photoreceptor, and the exchanger was activated by switching back to Na^+ solution. The resulting exchanger current yielded the number of Ca^{2+} ions that had entered the cell with the dark current and was used to calculate the fractional Ca^{2+} currrent. The results of this first study of fractional Ca^{2+} currents in CNG channels indicate that 15% of the dark current is carried by Ca^{2+} ions under physiological conditions. One concern is, however, that the use of Li^+ may have influenced the fractional Ca^{2+} current, and that the value in Na^+ solution may be different.

To investigate the dependence of P_f on the monovalent cation carrying the inward current together with Ca^{2+}, we exchanged extracellular Na^+ for Li^+ and recorded P_f values at four different Ca^{2+} concentrations. Figure 4D shows that P_f values obtained from bC with Li^+ were larger at all Ca^{2+} concentrations. This finding may either reflect a higher Ca^{2+} affinity in the presence of Li^+ or, alternatively, a lower rate of permeation by Li^+ compared with Na^+. Both effects would result in larger P_f values. To distinguish between the two possibilities, we compared amplitudes of macroscopic currents carried by Li^+ and Na^+ in outside-out patches from cells expressing bC at –70 mV and 1 mM cGMP with the same ion concentrations used in the P_f measurements. The ratio I_{Li}/I_{Na} of 0.34 ± 0.03 (nine patches; data not shown) indicates that Li^+ conductance is smaller than Na^+ conductance in bC channels, as reported earlier for other CNG channels (e.g. Menini, 1990; Frings *et al*., 1992; Nizzari *et al*., 1993; Eismann *et al*., 1994; Weyand *et al*., 1994; Haynes, 1995). If we assume that the Ca^{2+} affinity of the binding site is not affected by the exchange of Li^+ for Na^+, we can calculate theoretical values for $P_f(Li^+)$ using the measured current ratio:

$$P_f(Li^+) = \frac{P_f(Na^+)}{P_f(Na^+) + [1-P_f(Na^+)]\bullet \frac{I_{Li}}{I_{Na}}} \qquad (2)$$

We obtain a fair agreement of calculated and measured values (Figure 4D), suggesting that the reduced Li^+ conductance can largely account for the increased fractional Ca^{2+} current observed with extracellular Li^+. This analysis shows that the specific interaction of monovalent cations with the binding site in the channel pore also contributes to the fractional Ca^{2+} current in CNG channels. The affinity of the cation-binding site for Ca^{2+}, which is much higher than for monovalent ions, appears not to be altered upon exchanging Li^+ for Na^+, in agreement with the observation in rod photoreceptors that Ca^{2+} influx is largely unaffected by the monovalent cation prevalent in the external solution (Nakatani and Yau, 1988). However, differences in conductance between Na^+, K^+, Li^+, Rb^+ and Cs^+ demonstrated for all CNG channels (e.g. Yau and Nakatani, 1984; Menini, 1990; Frings *et al*., 1992; Baumann *et al*., 1994; Eismann *et al*., 1994; Weyand *et al*., 1994) modify the fractional Ca^{2+} current and have to be considered for the interpretation of P_f data.

For electrophysiological investigations of Ca^{2+} influx, intracellular K^+ is often replaced by Cs^+ to avoid activation of Ca^{2+}-dependent K^+ currents. We also used intracellular Cs^+ for our P_f measurements (see Materials and methods) and tested whether the use of Cs^+ altered P_f values. Comparing P_f values measured at 0.5 mM $[Ca^{2+}]_o$ with either K^+ or Cs^+, we obtained $P_f(K^+)/P_f(Cs^+)$ values of 0.88 ± 0.18 (6) for bC, 1.08 ± 0.19 (6) for bO and 0.98 ± 0.26 (3) for Dm (Figure 4B). In previous studies of CNG channels, it was noted that Cs^+ on the cytosolic side of the patch significantly reduced macroscopic inward currents carried by Na^+ or K^+ (Menini, 1990; Baumann *et al*., 1994; Eismann *et al*., 1994; Weyand *et al*., 1994). This effect of Cs^+ on the channel could be brought about by either of two mechanisms, namely a reduction of P_o or a decrease of single-channel current. If Cs^+ ions affect ion conduction they might also have influenced our P_f values. To test this possibility, we recorded bC single-channel currents at –50 mV from inside-out patches with either K^+ or Cs^+ on the cytosolic side. Figure 4C shows a channel displaying a P_o of 0.84 with K^+ and 0.33 with Cs^+ at 1 mM cGMP. At 15 μM cGMP, P_o was 0.37 with K^+ and 0.24 with Cs^+. The Cs^+ effect on P_o was reversed readily upon changing to K^+ solution. Single-channel current was only slightly affected (–0.79 pA with K^+ and –0.68 pA with Cs^+). The small difference probably arises from Cs^+-induced flickering between open and closed states that leads to underestimation of the channel current. These data show that intracellular Cs^+ lowers P_o in CNG channels and that P_f recorded with intracellular Cs^+ was measured at lower P_o than with intracellular K^+. Because intracellular Cs^+ does not affect ion conductance at –70 mV, it is not surprising that the fractional Ca^{2+} currents recorded with K^+ and Cs^+ are largely similar. These results also provide independent evidence that P_f does not significantly depend on the P_o of the channels under our recording conditions.

Modulation of P_f by membrane voltage and extracellular pH

Previous studies have revealed a pronounced voltage dependence of Ca^{2+} blockage in CNG channels (Colamartino *et al*., 1991; Root and MacKinnon, 1993; Zufall and Firestein, 1993; Eismann *et al*., 1994; Frings *et al*., 1995; Kleene, 1995; Seifert *et al*., 1999). In particular, a characteristic relief of Ca^{2+} blockage is observed at increasingly negative V_m. This relief has been attributed to a voltage-induced acceleration of Ca^{2+} exit to the cytosolic side of the pore. According to this concept, Ca^{2+} affinity must decrease upon hyperpolarization, and this should also reduce P_f. This prediction is borne out by the results shown in Figure 5A. The P_f values of bC at 0.3 mM $[Ca^{2+}]_o$ indeed decline with hyperpolarization, with mean values of 0.24 ± 0.04 (6) at –30 mV, and 0.07 ± 0.01 (3) at –90 mV. This result corroborates the correlation between Ca^{2+} affinity and fractional Ca^{2+} current and further strengthens the concept that factors that modulate Ca^{2+} binding to CNG channels also affect P_f.

The data gained from these experiments can be used to address a physiologically important question. How does the absolute Ca^{2+} current (I_{Ca}) through CNG channels depend on V_m? In two cells, we were able to measure P_f successively at four different voltages. Because these

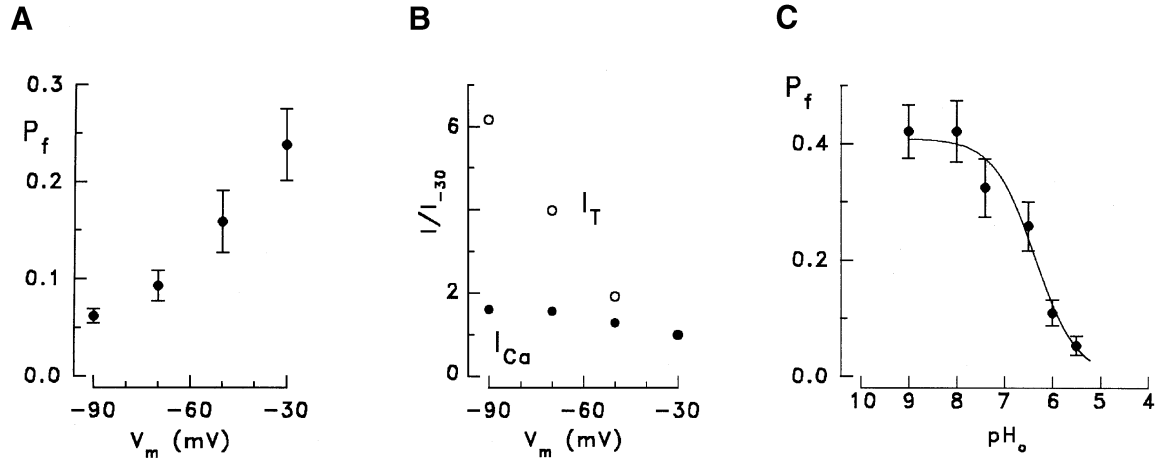

Fig. 5. Modulation of P_f by membrane voltage and extracellular pH. (**A**) Dependence of P_f on V_m for bC at 0.3 mM $[Ca^{2+}]_o$. Means and standard deviations of three to six cells for each voltage. (**B**) Voltage dependence of I_{Ca} relative to –30 mV calculated from four I_T and P_f values obtained at 0.3 mM $[Ca^{2+}]_o$ from a cell expressing bC (●); ○: the corresponding relative I_T values for the same cell. Absolute current amplitudes at –30 and –90 mV were –136 and –839 pA for I_T, and –32 and –52 pA for I_{Ca}. (**C**) Modulation of P_f by extracellular pH (pH_o). Acidification of the extracellular solution reduces P_f with an apparent pK of 6.37. Means of three to ten cells expressing bC with 1 mM $[Ca^{2+}]_o$ at –70 mV.

measurements were obtained from the same number of channels at similar P_o, we can calculate the absolute Ca^{2+} current from

$$I_{Ca} = I_T \cdot P_f \quad (3)$$

Figure 5B shows I_{Ca}, calculated according to Equation 3, and the total current I_T at four different V_m values between –30 and –90 mV. I_{Ca} increased only 1.6-fold (filled circles), whereas I_T increased 6-fold (open circles). Comparison of P_f, I_T and I_{Ca} in Figure 5A and B illustrates the consequences of hyperpolarization: acceleration of Ca^{2+} exit causes an apparent decrease in binding affinity and, thereby, a decrease in blocking efficiency and a decrease of P_f. As a result of reduced Ca^{2+} blockage, Na^+ current (and hence I_T) is strongly augmented, whereas the Ca^{2+} current is augmented to a much lesser extent. These data show that the balance between electrical and chemical signaling is shifted upon change of membrane voltage, due to a change in the apparent Ca^{2+} affinity of the channel.

Ca^{2+} affinity can also be modulated by the extracellular pH (pH_o). Root and MacKinnon (1994) showed that the glutamic acid residues that serve as cation-binding sites in the CNG channel pore can be protonated. In fact, protonation strongly reduces the Ca^{2+}-binding affinity (Seifert *et al*., 1999) and is, therefore, also expected to reduce P_f. The effect of pH_o on P_f at 1 mM $[Ca^{2+}]_o$ is illustrated for bC in Figure 5C. Acidification of the extracellular medium strongly decreases P_f from 0.42±0.05 (10) at pH_o 8.0 to 0.05±0.02 (3) at pH_o 5.5. This pH dependence could be fitted with a modified Hill equation:

$$P_f = P_f^{max} \bullet \left(1 - \frac{pH_o}{pH_o + pK_{app}} \right) \quad (4)$$

where P_f^{max} is the maximal P_f value for a specific combination of $[Ca^{2+}]_o$ and V_m. The apparent titration constant pK_{app} is the pH_o that induces half-maximal reduction of P_f. The data in Figure 5C were fitted with $P_f^{max} = 0.41$ and $pK_{app} = 6.37$. pK_{app} is an estimate for the pK of the binding site under the conditions used.

The effect of modulatory subunits on Ca^{2+} permeation

While it was demonstrated recently that CNG channels mediate an odor-induced Ca^{2+} influx into the sensory cilia of OSNs (Leinders-Zufall *et al*., 1997, 1998), the small size of the cilia makes P_f measurements impracticable. However, it was suggested recently that the native olfactory channel expressed in the sensory cilia of rat OSNs is composed of three subunits, CNCα3, CNCα4 and CNCβ1b (Sautter *et al*., 1998). CNCα3 is the rat homolog of bO (Dhallan *et al*., 1990), CNCα4 is a modulatory subunit identified in rat OSNs (Bradley *et al*., 1994; Liman and Buck, 1994), and CNCβ1b is a splice variant of the modulatory CNCβ1a subunit of rod photoreceptor channels in the rat (Chen *et al*., 1994; Körschen *et al*., 1995; Sautter *et al*., 1998). The glutamate residue in CNCα3 which contributes to the high-affinity Ca^{2+}-binding site of the channel is replaced by an aspartate in CNCα4 and by an uncharged glycine residue in CNCβ1b. We investigated how co-expression of CNCα3 with its modulatory subunits affects the fractional Ca^{2+} current. The analysis was performed at 0.5 and 2 mM $[Ca^{2+}]_o$ where bO shows P_f values of 0.21 and 0.67, respectively (Table I). We obtained slightly smaller P_f values with the rat ortholog CNCα3 (Figure 6A, α3): 0.16±0.02 (6) at 0.5 mM and 0.56±0.04 (11) at 2 mM. Combining CNCα3 and CNCα4 produced only a slight decrease of P_f (Figure 6A; α3α4). Co-expression of CNCα3 with CNCβ1b yielded P_f values ~30% lower than measured with homomers (Figure 6A; α3β1b), reflecting a decrease of Ca^{2+} affinity that is probably the consequence of replacing one or several glutamate residues by glycine in the binding site. When all three subunits were co-expressed (Figure 6A; α3α4β1b), P_f was slightly higher than with α3β1b, but the values are still ~25% lower than in the homomeric CNCα3 channels. These data show that the modulatory subunit CNCβ1 reduces Ca^{2+} affinity (cf. Körschen *et al*., 1995) and the fractional Ca^{2+} current in CNG channels.

Although P_f measurements with native olfactory channels presently are not feasible, we can obtain important information about the relationship between Ca^{2+} affinity

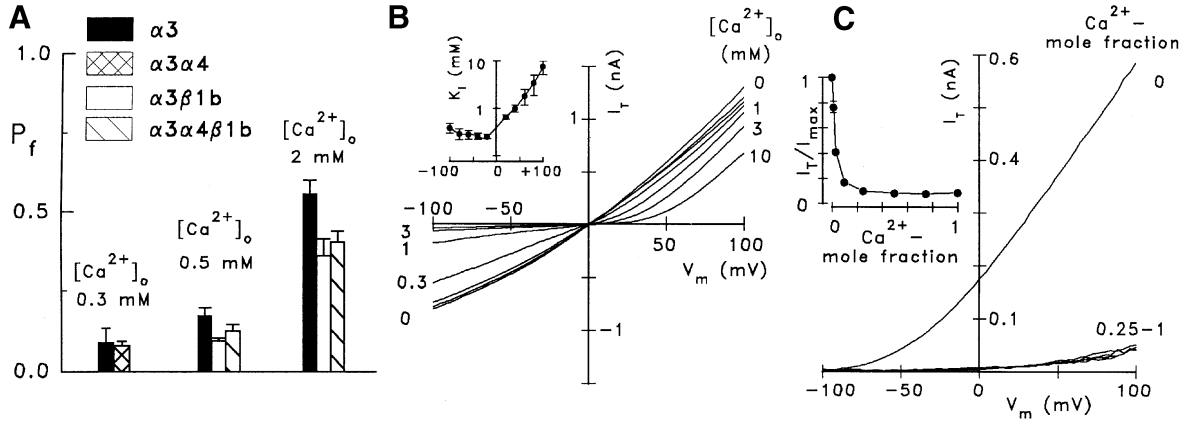

Fig. 6. Ca^{2+} permeation in heteromeric CNG channels. (**A**) The effect of modulatory subunits on Ca^{2+} permeation in the rat olfactory CNG channel. P_f was determined with cells expressing either CNCα3 homomers (α3, filled bars), heteromeric CNCα3/CNCα4 or CNCα3/β1b channels (α3α4, cross-hatched bar; α3β1b, open bars), or channels assembled from CNCα3, CNCα4 and CNCβ1b (α3α4β1b, hatched bars). P_f values at 0.3 mM Ca^{2+}: α3, 0.09±0.05 (8); α3α4, 0.08±0.01 (9). P_f values at 0.5 mM Ca^{2+}: α3, 0.17±0.02 (6); α3β1b, 0.10±0.01 (10); α3α4β1b, 0.13±0.02 (5). P_f values at 2 mM Ca^{2+}: α3, 0.56±0.04 (11); α3β1b, 0.36±0.05 (5); α3α4β1b, 0.41±0.03 (6). All measurements were done at –70 mV with 150 μM caged 8-Br-cGMP for α3 and α3β1b, with 75 μM caged cGMP for α3α4, and with 60 μM caged 8-Br-cGMP for α3α4β1b channels. (**B**) Ca^{2+} blockage in native olfactory channels from frog OSNs. I_T/V_m recordings from an outside-out patch of dendritic knob membrane with 100 μM cAMP in the pipette and various $[Ca^{2+}]_o$. Inset: voltage dependence of blocking constant K_i for extracellular Ca^{2+}. Means and standard deviations from three patches. (**C**) Voltage dependence of outward currents recorded at increasing Ca^{2+}-mole fractions from an inside-out patch of frog OSN dendritic knob membrane with the impermeable $NMDG^+$ in the pipette. Inset: dependence of the normalized residual current on Ca^{2+}-mole fraction. Means and standard deviation of five patches at +80 mV.

and Ca^{2+} conductance from native channels by analyzing Ca^{2+} blockage and Ca^{2+} currents at high Ca^{2+} concentrations. To study Ca^{2+} blockage, outside-out patches were obtained from dendritic knobs of freshly dissociated OSNs from the frog *Rana esculenta*, and I_T/V_m relationships were recorded at 140 mM $[Na^+]_o$ and various levels of $[Ca^{2+}]_o$. Figure 6B shows a family of I_T/V_m recordings, and the inset in Figure 6B illustrates the voltage dependence of the Ca^{2+}-blocking constant, K_i, derived from three patches. The mean K_i value at –70 mV is 285±65 μM $[Ca^{2+}]_o$, indicating that the Ca^{2+} affinity of the native frog olfactory channel is distinctly lower than observed with homomeric CNCα3 channels. A similar blocking constant recently was reported for olfactory sensory cilia of the frog *Rana pipiens* (K_i = 250 μM at –50 mV; Kleene, 1995; the small difference is accounted for mostly by the voltage difference, as we obtain a K_i of 265±45 μM at –50 mV). Together with the co-expression studies shown in Figure 6A, these results show that native olfactory CNG channels, consisting of principal and modulatory subunits, display lower Ca^{2+} affinity and P_f values than homomeric channels containing only the principal subunit.

To measure Ca^{2+} currents at high Ca^{2+} concentrations, we recorded cAMP-dependent outward currents from inside-out patches of frog OSN dendritic knobs at various Ca^{2+}-mole fractions {Ca^{2+}-mole fraction is defined as: $[Ca^{2+}]_i/([Ca^{2+}]_i + [Na^+]_i)$, with $[Ca^{2+}]_i + [Na^+]_i$ = 100 mM}, in the absence of permeable ions on the extracellular side of the patches. The voltage dependence of outward currents shown in Figure 6C illustrates the strong suppression of I_T by Ca^{2+} to a small residual amplitude at Ca^{2+}-mole fractions of 0.25–1. The dependence of the residual current on the a Ca^{2+}-mole fraction is presented in the inset of Figure 6C: at a Ca^{2+}-mole fraction of 1, where Ca^{2+} is the only permeable ion species, the residual current does not decline to <8–9% of the Na^+ current measured in Ca^{2+}-free solution. This value is clearly higher than found under similar conditions for the native rod photoreceptor CNG channel of the tiger salamander *Ambystoma tigrinum* (1.2%; Colamartino *et al.*, 1991). Thus, Ca^{2+} permeation in native olfactory CNG channels is distinctly more pronounced than in native rod photoreceptor channels. This finding is in good accordance with the observation that bO shows a stronger relief of Ca^{2+} blockage at negative potentials than bR (Frings *et al.*, 1995). Both lines of evidence demonstrate that olfactory channels conduct Ca^{2+} more efficiently than rod photoreceptor channels, and that this increased Ca^{2+} permeation is associated with lower binding affinity for extracellular Ca^{2+}.

Discussion

The relationship between Ca^{2+} affinity and fractional Ca^{2+} current

Our studies of Ca^{2+} blockage and fractional Ca^{2+} currents in four different CNG channel types have revealed a simple relationship between Ca^{2+} affinity and fractional Ca^{2+} current: CNG channels with high affinity display high P_f values, while low-affinity channels have low P_f values. The correlation of K_i and K_{Pf} is illustrated in Figure 7A for the four channel types investigated here: in bR, high blocking efficiency (a small value of K_i) leads to high P_f values at submillimolar $[Ca^{2+}]_o$ (a small value of K_{Pf}), while the weak blockage in Dm coincides with a 10-fold higher K_{Pf}. Furthermore, a correlation between Ca^{2+} affinity and Ca^{2+} permeation can be derived from current measurements at high concentrations (73–220 mM) of either Na^+ or Ca^{2+} as charge carriers: in the high-affinity rod photoreceptor channel, amplitudes of Ca^{2+} currents reach only ~1% of Na^+ currents (Colamartino *et al.*, 1991), while 8–11% are observed with the low-affinity channels of frog OSNs and *Drosophila* (Baumann *et al.*, 1994; this study).

We have demonstrated the interdependence of affinity, permeation and fractional Ca^{2+} current in a simple experi-

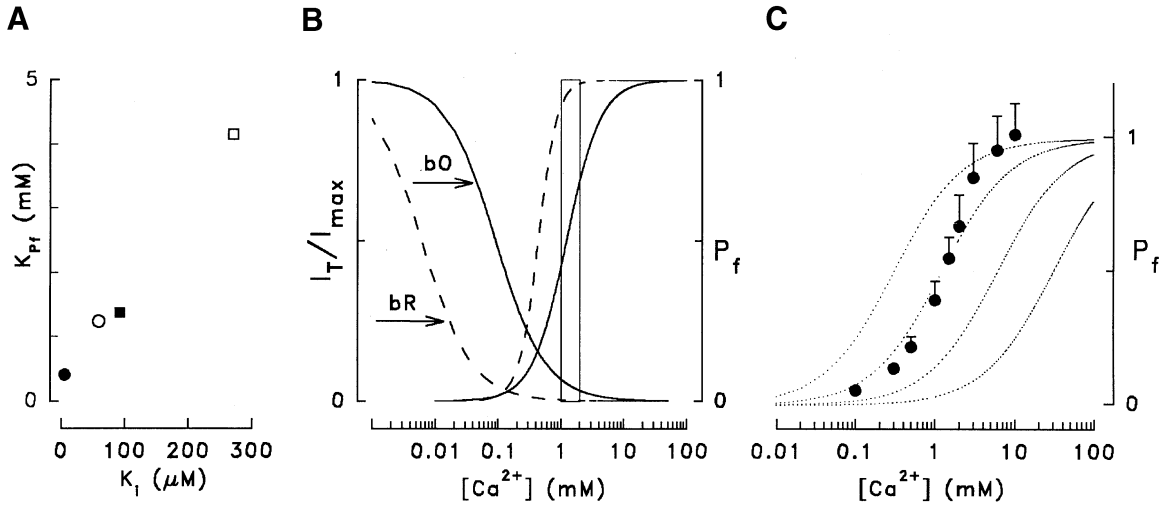

Fig. 7. Ca^{2+} affinity, fractional Ca^{2+} current and Ca^{2+} permeation in CNG channels. (**A**) Relationship between the blocking constants for extracellular Ca^{2+}, K_i and the P_f constants, K_{Pf}, at –70 mV. Values are from bR (●), bO (○), bC (■) and Dm (□). (**B**) Comparison of Ca^{2+} blockage and fractional Ca^{2+} current, P_f, for bR (dashed lines) and bO (solid lines) at –70 mV. Ca^{2+} blockage is illustrated as the fraction of the total current, I_T, that remains unblocked in the presence of the indicated $[Ca^{2+}]_o$. I_{max} is the current in Ca^{2+}-free solution (blocking data from Frings *et al*., 1995). (**C**) Comparison of the Ca^{2+} dependence of P_f (data from Figure 3) with the GHK model. Lines were constructed using Equation 5 with V_m = –70 mV and the following values for the relative cation permeability P_M/P_{Ca}: 0.01, 0.02, 0.1 and 0.5.

ment (Figure 5A and B): hyperpolarizing the membrane accelerates Ca^{2+} permeation and decreases the apparent Ca^{2+} affinity (Colamartino *et al*., 1991; Frings *et al*., 1995; Seifert *et al*., 1999). Such a reduction in Ca^{2+} affinity is expected also to reduce P_f, as suggested by the correlation shown in Figure 7A. We indeed observe a strong suppression of P_f upon hyperpolarization which confirms that manipulations which decrease Ca^{2+} affinity also increase Ca^{2+} permeation and reduce the fractional Ca^{2+} current. This voltage dependence of P_f sets CNG channels apart from other channels that conduct mixed cation currents. In particular, P_f in glutamate receptor channels does not change with voltage between –30 and –90 mV (Schneggenburger *et al*., 1993; Burnashev *et al*., 1995; Garashuk *et al*., 1996; Schneggenburger, 1996), and P_f increases upon hyperpolarization in acetylcholine receptors (Zhou and Neher, 1993). In these channels, where P_f is not determined by competition of Ca^{2+} and monovalent cations for a single binding site, currents carried by Ca^{2+} and Na^+ are augmented by hyperpolarization to a similar extent.

In CNG channels, the determining factor for both Ca^{2+} blockage and Ca^{2+} permeation is the binding affinity of the intrapore binding site for extracellular Ca^{2+}. High-affinity binding favors the selection of Ca^{2+} over Na^+, even in solutions where $[Na^+]_o$ is 100-fold higher than $[Ca^{2+}]_o$, giving rise to high blocking efficiency and high P_f values at physiological levels of $[Ca^{2+}]_o$. Ca^{2+} permeation, on the other hand, is slowed down because high-affinity binding decelerates dissociation of Ca^{2+} ions to the cytosolic exit of the channel. Thus, a CNG channel with high Ca^{2+} affinity constitutes a 'sticky pore' where Ca^{2+} permeation is limited by a relatively long dwell time at the intrapore binding site. In such channels, monovalent currents are strongly suppressed already at low Ca^{2+} concentrations, and P_f values are high.

The physiological consequence of this relationship is illustrated in Figure 7B using the examples of bR (K_i = 6 μM; K_{Pf} = 0.41 mM) and bO (K_i = 92 μM; K_{Pf} = 1.24 mM). Inspection of the data for bR (dashed lines) within the boxed-in concentration range (1–2 mM $[Ca^{2+}]_o$) shows that P_f has reached almost unity, while a very small residual current (<1% of I_{max}) supports only a small Ca^{2+} influx ($I_{Ca} = I_T \bullet P_f$). In contrast, the residual current of bO channels (solid lines) is ~5% of I_{max} with P_f values of ~0.6. Thus, bO channels (and also bC channels which have a similar Ca^{2+} dependence) conduct more Ca^{2+} than bR channels at 1–2 mM $[Ca^{2+}]_o$ because I_T is >5-fold higher while P_f is smaller by only 40%.

The interrelationship of Ca^{2+} affinity, P_f and Ca^{2+} permeation discussed above illustrates the differences in ion permeation between the four CNG channels investigated here. However, under certain conditions, a decrease of Ca^{2+} affinity and P_f can be associated with reduced instead of augmented Ca^{2+} permeation. This is demonstrated by our pH experiments: acidification strongly reduces I_T and Ca^{2+} affinity (Seifert *et al*., 1999) and, at the same time, the fractional Ca^{2+} current (this study). With small I_T and small P_f, Ca^{2+} permeation is also small at low pH, despite a diminished Ca^{2+} affinity. This observation cannot be explained by the 'sticky pore' concept in which Ca^{2+} permeation is controlled solely by the Ca^{2+} exit rate from the binding site. The pH effects illustrate a change in the rate with which ions enter the channel pore. At low pH, when the glutamate residues of the binding site show a higher degree of protonation, entry of both Ca^{2+} and Na^+ is decelerated, giving rise to a suppression of I_T. The decline of P_f values with acidification suggests that Ca^{2+} entry is hindered more efficiently than Na^+ entry. In conclusion, with data about Ca^{2+} affinity and fractional Ca^{2+} current, it is possible to predict how efficiently a CNG channel conducts Ca^{2+} ions under standard physiological conditions. However, factors that influence cation entry into the channel pore have to be considered as co-determinants of Ca^{2+} permeation.

Information about the molecular processes that underlie Ca^{2+} permeation in CNG channels can also be derived from inspection of the Ca^{2+} dependence of the fractional

Ca^{2+} current. Figure 7C shows that it is not possible to fit the Ca^{2+} dependence of P_f using the Goldman–Hodgkin–Katz (GHK) equation for electrodiffusion across biological membranes (Equation 5 in Materials and methods). The GHK equation yields relationships of P_f and $[Ca^{2+}]_o$ that are not steep enough to fit the P_f data in any of the CNG channels analyzed. Such deviation from the GHK model is often interpreted as evidence for ionic interactions within a pore that accommodates more than one ion. In fact, previous work has suggested that two monovalent cations can be bound within the pore of CNG channels at the same time (Sesti *et al*., 1995). As proposed earlier (Frings *et al*., 1995), entry of a second Ca^{2+} ion may displace a Ca^{2+} ion already bound which can then exit the channel to the cytosolic side. Electrostatic repulsion between two Ca^{2+} ions inside the pore may, therefore, be crucial for supporting high rates of Ca^{2+} permeation. Although there is no additional independent evidence for double occupancy by Ca^{2+} ions yet, it represents an attractive concept for the explanation of the shape of P_f/$[Ca^{2+}]_o$ relationships, which is based on the similarities between CNG channels and voltage-gated Ca^{2+} channels for which this scheme of Ca^{2+} permeation was developed (Tsien *et al*., 1987; McCleskey, 1994; Dang and McCleskey, 1998).

Comparison of CNG channels and voltage-gated Ca^{2+} channels

Comparison of similarities and differences between CNG channels and voltage-gated Ca^{2+} channels can help to understand the permeation mechanism in CNG channels. In homomeric CNG channels and in voltage-gated Ca^{2+} channels, a set of four glutamate residues forms the cation-binding site in the pore (Kim *et al*., 1993; Tang *et al*., 1993; Yang *et al*., 1993; Ellinor *et al*., 1995). Both channels conduct monovalent cations in the absence of Ca^{2+}, showing values of single-channel conductance in the range of 20–80 pS in Ca^{2+}-free solution. Micromolar concentrations of extracellular Ca^{2+} block monovalent currents in both channel types, but voltage-gated Ca^{2+} channels show higher Ca^{2+} affinity (K_i of ~1 μM) compared with CNG channels (K_i values in the range of 6–300 μM). In both channel types, Ca^{2+} permeation may be accelerated by mutual repulsion of Ca^{2+} ions in the doubly occupied pore, as suggested by deviation from the GHK theory for CNG channels (Frings *et al*., 1995; this study), and by observation of anomalous mole-fraction behavior with voltage-gated Ca^{2+} channels (Tsien *et al*., 1987). Finally, current recordings at high concentrations of the charge carriers have revealed a similar efficiency of Ca^{2+} permeation: the single-channel conductance of voltage-gated Ca^{2+} channels from ventricular heart cells is 85 pS with 150 mM Na^+ and 9 pS with 110 mM Ca^{2+} (Hess *et al*., 1986). Such a relative Ca^{2+}/Na^+ conductance of 10% is also observed with native olfactory CNG channels and homomeric Dm channels. While these similarities in pore structure and conducting properties point to a common mechanism for ion permeation, some dissimilarities illustrate the different tasks that the two channel types fulfill under physiological conditions. First, the higher Ca^{2+} affinity of voltage-gated Ca^{2+} channels causes a virtually complete suppression of monovalent currents and produces pure Ca^{2+} currents at 1–2 mM $[Ca^{2+}]_o$, whereas the known native CNG channels conduct mixed cation currents at this $[Ca^{2+}]_o$ (Nakatani and Yau, 1988; Perry and McNaughton, 1991). Secondly, both channel types can co-assemble with various modulatory subunits, but while the high-affinity binding site is preserved in voltage-gated Ca^{2+} channels (De Waard *et al*., 1996), glycine residues reduce Ca^{2+} affinity in heteromeric CNG channels. Thirdly, despite their high Ca^{2+} affinity, voltage-gated Ca^{2+} channels conduct substantial Ca^{2+} currents, possibly sustained by electrostatic repulsion of two Ca^{2+} ions that can occupy the pore at the same time. Such a mechanism appears to be much less effective in CNG channels, although double occupancy may also play a role. However, high Ca^{2+} affinity in CNG channels is clearly correlated with low Ca^{2+} conductance, and the most substantial Ca^{2+} influx is mediated by low-affinity channels, and is associated with equally substantial Na^+ influx. In conclusion, several structural features common to both channel types give rise to pure Ca^{2+} currents in voltage-gated Ca^{2+} channels and to mixed cation currents with a high Ca^{2+} fraction in CNG channels.

Modulatory subunits increase Ca^{2+} permeation in native CNG channels

While there is preliminary evidence that CNG channels may form homomeric proteins *in situ* (Wiesner *et al*., 1998), a number of studies with various tissues and expression systems have clearly demonstrated that native CNG channels can form heteromeric protein complexes consisting of principal subunits (CNCα1, CNCα2 or CNCα3) plus one or more modulatory subunits. Native rod photoreceptor CNG channels contain both CNCα1 and CNCβ1a (Chen *et al*., 1994; Körschen *et al*., 1995). CNCα2 is co-localized with a different splice form of CNCβ1 in bovine sperm cells (Wiesner *et al*., 1998), and CNCα3 co-assembles in olfactory cilia with CNCα4 and CNCβ1b. Co-assembly of the three subunits confers high cAMP sensitivity to the olfactory channel ($K_{1/2}$ = 4 μM; Frings *et al*., 1992) and reduces the single-channel conductance in Ca^{2+}-free solution from 33 to 21 pS (W.Bönigk, F.Sesti, J.Bradley, F.Müller, G.V.Ronnett, U.B.Kaupp and S.Frings, submitted). All known splice forms derived from the CNCβ1 gene contain a glycine residue in the position that corresponds to the Ca^{2+}-binding site in the principal subunits (Chen *et al*., 1994; Körschen *et al*., 1995; Biel *et al*., 1996b; Wiesner *et al*., 1998). The replacement of one or more negatively charged glutamates in this critical position by uncharged residues reduces Ca^{2+} affinity (Root and MacKinnon, 1993; Eismann *et al*., 1994; Körschen *et al*., 1995). We have shown here that the co-assembly of CNCα3 with CNCβ1b strongly reduces P_f at 0.5 and 2 mM $[Ca^{2+}]_o$, i.e. it increases the P_f constant K_{Pf}. Our results show that Ca^{2+} blockage and Ca^{2+} permeation strongly depend on the set of subunits expressed in an individual cell type. Recent evidence suggests that all known CNG channel subunits can co-assemble, giving rise to a large diversity of heteromeric channel proteins (Finn *et al*., 1998). With all possible combinations of subunits, the CNG channel family offers a large repertoire of Ca^{2+}-permeable channels, ranging from homomeric CNCα1 channels with a very low Ca^{2+} conductance, to channels with substantial Ca^{2+} permeation that may be homomers of CNCα2 or CNCα3, or heteromeric proteins

containing a splice form of CNCβ1. Analysis of the exact set of subunits expressed by a cell population, therefore, provides information about the significance of cyclic nucleotide-induced Ca^{2+} signals in cellular information processing.

Physiological implications of differences in Ca^{2+} affinity

In recent years, a large number of studies reported detection of CNG channel subunits in various cell populations by *in situ* hybridization or immunochemistry (e.g. Nawy and Jahr, 1990; Dryer and Henderson, 1991; Ahmad *et al*., 1994; Biel *et al*., 1994; Distler *et al*., 1994; El-Husseini *et al*., 1995; Leinders-Zufall *et al*., 1995; Bönigk *et al*., 1996; Kingston *et al*., 1996; Bradley *et al*., 1997; Misaka *et al*., 1997; Sautter *et al*., 1997; Thompson, 1997; Wiesner *et al*., 1998). In the following, we discuss possible predictions for Ca^{2+} signaling that can be made based on the analysis of cell-specific expression of the principal subunits (CNCα1, CNCα2 and CNCα3).

Because of their high Ca^{2+} affinity, homomeric CNCα1 channels conduct only small currents that are carried mainly or exclusively by Ca^{2+} ions. As cyclic nucleotide-gated (CNG) Ca^{2+} channels, their contribution to Ca^{2+} signaling would be much more pronounced than their effect on membrane voltage. Although their Ca^{2+} conductance is low compared with voltage-gated Ca^{2+} channels, the channels can mediate considerable Ca^{2+} influx because they show no intrinsic inactivation and can, therefore, conduct persistent Ca^{2+} currents at hyperpolarized voltages. Homomeric channels composed of either CNCα2 or CNCα3 subunits are blocked less efficiently at physiological $[Ca^{2+}]_o$ and conduct larger depolarizing currents carried at roughly equal fractions by Na^+ and Ca^{2+}. Ca^{2+} influx is rapid, because Ca^{2+} ions bind less tightly to the pore, and transfer rates approach those reported for voltage-gated Ca^{2+} channels. Activation of these channels will, consequently, cause both marked depolarization and a pronounced increase of cytosolic $[Ca^{2+}]$. The balance of electrical and chemical signaling critically depends on $[Ca^{2+}]_o$, as the Ca^{2+} dependence of P_f is very steep. Therefore, the relative contribution of either signal is difficult to assess, if the free $[Ca^{2+}]_o$ is not known as, for example, in OSNs.

Interestingly, the *Drosophila* channel investigated here shows the lowest Ca^{2+} affinity and the highest P_f constant, precisely matching the difference in extracellular Ca^{2+} concentration between interstitial fluids of vertebrates (1–3 mM) and the hemolymph of flies (7–10 mM; Ashburner, 1989). This suggests that the Dm channel has a similar task in cellular signaling in *Drosophila* to that of CNCα2 and CNCα3 have in vertebrates, namely the generation of simultaneous voltage and Ca^{2+} signals upon a rise in cGMP concentration.

In addition to subunit composition, we have identified several factors that may affect Ca^{2+} affinity and, hence, Ca^{2+} permeation *in situ*. (i) The extracellular pH is an important co-determinant for Ca^{2+} permeation in homomeric CNG channels, since acidification strongly reduces Ca^{2+} affinity and the fractional Ca^{2+} current through protonation of the intrapore binding site. However, the effects of protonation are complex since both I_{Na} and I_{Ca} are reduced. Furthermore, pH effects on heteromeric channels have not been studied and may differ considerably from channels containing only principal subunits. In fact, the native CNG channels from frog OSNs appears to be largely insensitive to changes in pH_o (Frings *et al*., 1992). Consequently, pH effects on Ca^{2+} permeation have to be investigated for each subunit composition expressed in a particular cell. (ii) The membrane voltage should be considered as a factor that balances the contributions of electrical and chemical signaling, as the fractional Ca^{2+} current strongly decreases upon hyperpolarization. This is particularly interesting because CNG channels can operate over a much wider range of membrane voltages than voltage-gated Ca^{2+} channels (e.g. –30 to –80 mV in photoreceptors). (iii) The fractional Ca^{2+} current is determined by the contributions of all ion species conducted by a channel. We have shown that the exchange of Li^+ for Na^+ changes P_f values to an extent that reflects differences in conductance between the two monovalents. Under physiological conditions, other permeable ions may influence P_f and, in particular, contributions of Mg^{2+} and K^+ should be studied. Mg^{2+} has been shown to have high binding affinity and limited permeability in CNG channels (e.g. Nakatani and Yau, 1988; Zimmermann and Baylor, 1992; Baumann *et al*., 1994; Frings *et al*., 1995), and K^+ ions may contribute significant outward currents at depolarized membrane voltages (for example in photoreceptors) or inward currents at elevated $[K^+]_o$ (for example in OSNs where $[K^+]_o$ is 69 mM; Reuter *et al*., 1998). (iv) Finally, changes of $[Ca^{2+}]_o$ will affect Ca^{2+} permeation, as P_f shows the steepest Ca^{2+} dependence within the physiological range of $[Ca^{2+}]_o$. Such changes are expected to occur in cells where high densities of CNG channels cause local depletion of extracellular Ca^{2+}. Channel densities found in rod photoreceptors (~300/μm^2; Haynes *et al*., 1986; Zimmerman and Baylor, 1986) and olfactory cilia (200–400/μm^2; Kleene, 1994) may warrant an investigation of possible effects of local Ca^{2+} depletion that would relieve Ca^{2+} blockage and reduce Ca^{2+} permeation.

Materials and methods

Heterologous expression of CNG channels

For transient expression of bovine CNCα1 and CNCα3, HEK-293 cells were transfected by calcium phosphate co-precipitation (Chen and Okayama, 1987) with pcDNAI (Invitrogen) containing the respective CNG channel cDNA, as described previously (Baumann *et al*., 1994). To enhance expression efficiency, the plasmid pRSV-Tag (Dhallan *et al*., 1990) was added, and co-expression of green fluorescent protein (GFP; Prasher *et al*., 1992; kindly provided by Professor P.Seeburg, Heidelberg) allowed optical identification of transfected cells. For experiments with bovine CNCα2 and DmCNC, HEK-293 cells were stably transfected using pcDNAIneo (Invitrogen) for CNCα2, and pTMT (kindly provided by Professor O.Pongs, Hamburg) for DmCNC. Voltage-gated N-type Ca^{2+} channels from rabbit brain (Fujita *et al*., 1993) were transiently expressed in HEK-293 cells using the pKCR vector (kindly provided by Dr J.Fujita, Tokyo) as described earlier (Frings *et al*., 1995).

Determination of the fractional Ca^{2+} current P_f in CNG channels

The contribution of Ca^{2+} to the current conducted by ion channels, P_f, can be measured by recording the total current with a patch pipette and, simultaneously, Ca^{2+} entry with a Ca^{2+}-sensitive dye (Neher and Augustine, 1992; Schneggenburger *et al*., 1993; Trouslard *et al*., 1993; Zhou and Neher, 1993; Vernino *et al*., 1994; Burnashev *et al*., 1995; Frings *et al*., 1995; Garaschuk *et al*., 1996; Schneggenburger, 1996; Tempia *et al*., 1996; Zeilhofer *et al*., 1997). We applied this method to

CNG channels using photolysis of caged cGMP and caged 8-Br-cGMP to achieve rapid channel activation. Transfected HEK-293 cells were grown on coverslips and transferred to the recording chamber with standard extracellular solution that contained (mM) 120 NaCl, 3 KCl, 50 glucose, 10 HEPES (pH 7.4), and $CaCl_2$ as indicated. The chamber was mounted on the stage of a Nikon Diaphot 300 inverted microscope and viewed through an oil immersion objective (Nikon Fluor 40×, na: 1.3 mm). Epifluorescence illumination was achieved by a Y-shaped UV light guide (AMKO, Tornesch, Germany). One input of the light guide was connected to a 75 W Xe lamp equipped with a computer-controlled filter wheel (Life Science Resources, Cambridge, UK), the second input was connected to a 100 W Hg lamp (AMKO) with built-in IR and UV filters (WG335, AMKO) and an electronically actuated shutter. The Xe lamp was used for fluorescence excitation of GFP (λ_{exc} = 450–490 nm, dichroic mirror: 510 nm, λ_{em} = 520–560 nm; Nikon) and FURA-2 (λ_{exc} = 340 or 380 nm, dichroic mirror: 400 nm, λ_{em} = 510 nm; Omega Optical, USA). The light of the Hg lamp was reflected into the objective by the 400 nm dichroic mirror to induce photolysis of caged compounds. To permit measurements of FURA-2 fluorescence without inducing photolysis, the Xe light was passed through a quartz neutral-density filter (ND = 2.0, Ealing Electro Optics, UK).

Cells were loaded in the whole-cell configuration of the patch-clamp technique (Hamill *et al*., 1981) by equilibration with standard pipette solution that contained (mM) 130 CsCl, 20 TEA-Cl, 2 $MgCl_2$, 2 Na_2-ATP, 0.2 Na_2-GTP, 0.02 EGTA, 10 HEPES (pH 7.2), 1–2 mM FURA-2-K_5 (Molecular Probes, Eugene, OR) and caged compounds. Cs^+ and TEA^+ were used to block K^+ currents that are activated by Ca^{2+} entry in HEK-293 cells. In a few experiments at $[Ca^{2+}]_o \leqslant 0.5$ mM, Cs^+ was replaced by K^+. Concentrations of caged cGMP or caged 8-Br-cGMP (Hagen *et al*., 1996) were: 150 μM caged cGMP for bC ($K_{1/2}$ = 17 μM); 120 μM caged 8-Br-cGMP for bR ($K_{1/2}$ = 9.5 μM); 75 μM caged cGMP for bO ($K_{1/2}$ = 1.5 μM); 150 μM caged cGMP for Dm ($K_{1/2}$ = 12.4 μM). Cell loading was confirmed by monitoring FURA-2 fluorescence. After equilibration (6–10 min after establishing the whole-cell configuration), the free Ca^{2+} concentration $[Ca^{2+}]_i$ was determined from the fluorescence ratio (F_{340}/F_{380}; Grynkiewicz *et al*., 1985). Cells were only used for P_f measurements if $[Ca^{2+}]_i$ was <200 nM at the end of the loading period. Cells were voltage clamped at –70 mV, and the total current I_T was recorded after photolysis of the caged ligands. Ca^{2+} entry was monitored by recording changes in the fluorescence intensity of FURA-2 (ΔF_{380}) using a photon counter system (PhoCal, Life Science Resources). Fluorescence intensity was normalized using fluorescent beads (1 BU = 1 bead unit), as described earlier (Frings *et al*., 1995). For the calculation of P_f, it is necessary to ascertain that the change in F_{380} is caused exclusively by Ca^{2+} entry through CNG channels, and does not reflect Ca^{2+} sequestration, Ca^{2+} release or saturation of the dye. If Ca^{2+} entry is the only cause for changes of F_{380}, the fluorescence signal must be strictly proportional to the number of Ca^{2+} ions entering the cell and, hence, to the current intergral $\int I_T dt$ (Neher and Augustine, 1992). The proportionality of F_{380} and $\int I_T dt$, therefore, was tested by superimposing the appropriately scaled current integral on the fluorescence trace. In all experiments, the calculation of P_f was restricted to the time interval for which proportionality was confirmed by this analysis. The result of such experiments is the proportionality constant $f = \Delta F_{380}/\int I_T dt$ that indicates the extent of fluorescence change due to the total current I_T conducted by CNG channels.

To derive the fractional Ca^{2+} current P_f from the measured value of f, it is necessary to establish the quantitative relationship between changes of F_{380} and the underlying Ca^{2+} current I_{Ca}. We obtained this relationship from measurements with HEK-293 cells expressing N-type Ca^{2+} channels (Frings *et al*., 1995). Channels were activated by a depolarizing voltage pulse, current (I_{Ca}) and fluorescence (F_{380}) were recorded, and the calibration constant $f_{max} = \Delta F_{380}/\int I_{Ca} dt$ was calculated. f_{max} values were determined routinely at 2 mM $[Ca^{2+}]_o$. Using the f value measured in each experiment and the calibration constant f_{max}, we obtained the fractional Ca^{2+} current according to $P_f = f/f_{max}$.

For comparison of P_f measurements with the GHK model, the dependence of P_f on $[Ca^{2+}]_o$ was calculated using the equation

$$P_f = \frac{4 \cdot [Ca^{2+}]_o}{4 \cdot [Ca^{2+}]_o + \frac{P_M}{P_{Ca}} [M^+]_o \{1 - \exp(2\psi)\}} \quad (5)$$

where P_M/P_{Ca} is the permeability for monovalent cations relative to Ca^{2+}, $[M^+]_o$ the extracellular concentration of monovalents, and $\psi = V_m F/RT$ (F is the Faraday constant, R the molar gas constant, T the absolute temperature).

The P_o of CNG channels can be adjusted in a P_f experiment by controlled photorelease of cGMP. We previously have shown that the concentration of cGMP liberated by a UV flash in a cell expressing CNG channels can be determined if the flash-induced current is compared with the current at maximal activation of the channels (Hagen *et al*., 1996). For the P_f measurements at low and high P_o, cells expressing bO were loaded with 75 μM caged cGMP, and test flashes of either 20 or 100 ms were applied. Channels were activated maximally by subsequent illumination for 1 s, and the P_o was derived from the ratio of test current to maximal current. With 20 ms flashes, I_{20}/I_{max} was 0.14±0.06 (4), reflecting a concentration of 0.9 μM photoreleased cGMP. With 100 ms test flashes, I_{100}/I_{max} was 0.94±0.10 (6), corresponding to ~4 μM liberated cGMP.

For single-channel recordings with cells expressing bC, pipettes were filled with standard extracellular solution containing 1 mM EGTA. Excised inside-out patches with single CNG channels were exposed consecutively to solutions containing as main cation either K^+ (145 mM KCl, 8 mM NaCl, 1 mM EGTA, 10 mM HEPES, pH 7.2) or Cs^+ (130 mM CsCl, 1 mM EGTA, 10 mM HEPES, pH 7.2). Channel currents were recorded at 15 and 1000 μM cGMP (V_m = –50 mV), and P_o was derived from amplitude histograms of 30 s segments of recording digitized at 3 kHz and filtered at 1 kHz.

The effect of pH_o on P_f was investigated using an extracellular solution (120 mM NaCl, 3 mM KCl, 50 glucose) that was adjusted to the appropriate pH_o using 10 mM of either MES (Sigma; pH_o 5.5–6.5), HEPES (Sigma; pH_o 7.4) or TAPS (Sigma; pH_o 8.0–9.0).

Co-expression studies of rat CNCα3, CNCα4 and CNCβ1b were performed as described elsewhere (W.Bönigk, F.Sesti, J.Bradley, F.Müller, G.V.Ronnett, U.B.Kaupp and S.Frings, submitted). The solutions for co-transfection contained the following molar ratios of plasmids CNCα3:CNCα4:CNCβ1b = 2:1:2. Molar ratios of CNCα3:CNCα4 and CNCα3:CNCβ1b were 1:1. The cells expressed almost homogeneous populations of channels, as confirmed by single-channel analysis. For recordings from native olfactory channels, OSNs were dissociated from frog olfactory epithelium as described previously (Frings *et al*., 1992). Briefly, epithelia were dissected and washed in Ringer′s solution containing 120 mM NaCl, 4 mM NaOH, 3 mM KCl, 1 mM $CaCl_2$, 2 mM $MgCl_2$, 5 mM glucose, 5 mM Na-pyruvate, 10 mM HEPES, pH 7.4. After incubation with 1 mg/ml papain (Sigma) in Ringer′s solution for 45 min at 35°C, the tissue was washed for 45 min at room temperature in dissociation solution containing 120 mM *N*-methyl-D-glucamine (NMDG)-Cl, 3 mM KCl, 5 mM glucose, 5 mM Na-pyruvate, 2 mM EDTA, 10 mM HEPES, pH 7.4. OSNs were isolated by trituration and patches obtained from dendritic knobs. The pipet solution for outside-out patches contained 120 mM NaCl, 20 mM NaOH, 10 mM EGTA, 10 mM HEPES, pH 7.2, and 100 μM cAMP. The bath solution was 130 mM NaCl, 4 mM NaOH, 10 mM HEPES, plus 1 EGTA and 1.05 mM $CaCl_2$ for 100 μM free Ca^{2+}, and no EGTA and the indicated amount of $CaCl_2$ for higher Ca^{2+} concentrations. Leak currents were estimated by measuring inward currents with the impermeable cation NMDG at –80 to –100 mV and linear extrapolation over the whole voltage range. Patches were only analyzed if leak currents were <5% of I_{max} (recorded in Ca^{2+}-free Na^+ solution). The pipet solution for inside-out patches contained 120 mM NMDG-Cl, 5 mM EGTA, 10 mM HEPES, pH 7.4. The bath solutions for the mole-fraction experiments contained NaCl and $CaCl_2$ at a total concentration of 100 mM, together with 10 mM HEPES, 6.5 mM Tris; pH 7.2 and 100 μM cAMP. Control currents were recorded separately for each mole-fraction and subtracted.

Acknowledgements

We gratefully acknowledge the assistance of Mechthilde Bruns, Helga Vent and Helmut Erkens. We thank Dr Arnd Baumann for the cell lines expressing CNCα2 and Dm, and Dr Reinhard Seifert for valuable comments on the manuscript. This work was supported by a grant of the Studienstiftung des Deutschen Volkes (to C.D.) and the Deutsche Forschungsgemeinschaft (grant FR 937 to S.F., and SFB 246).

References

Ahmad,I., Leinders-Zufall,T., Kocsis,J.D., Shepherd,G.M., Zufall,F. and Barnstable,C.J. (1994) Retinal ganglion cells express a cGMP-gated cation conductance activatable by nitric oxide donors. *Neuron*, **12**, 155–165.

Altenhofen,W., Ludwig,J., Eismann,E., Kraus,W., Bönigk,W. and Kaupp,U.B. (1991) Control of ligand specificity in cyclic nucleotide-gated channels from rod photoreceptors and olfactory epithelium. *Proc. Natl Acad. Sci. USA*, **88**, 9868–9872.

Ashburner,M. (1989) *Drosophila: A Laboratory Handbook*. Cold Spring Harbor Laboratory Press, Cold Spring Harbor, NY.

Baumann,A., Frings,S., Godde,M., Seifert,R. and Kaupp,U.B. (1994) Primary structure and functional expression of a *Drosophila* cyclic nucleotide-gated channel present in eyes and antennae. *EMBO J.*, **13**, 5040–5050.

Biel,M., Zong,X., Distler,M., Bosse,E., Klugbauer,N., Murakami,M., Flockerzi,V. and Hofmann,F. (1994) Another member of the cyclic nucleotide-gated channel family, expressed in testis, kidney and heart. *Proc. Natl Acad. Sci. USA*, **91**, 3505–3509.

Biel,M., Zong,X. and Hofmann,F. (1996a) Cyclic nucleotide-gated cation channels. Molecular diversity, structure and cellular functions. *Trends Cardiovasc. Med.*, **6**, 274–280.

Biel,M., Zong,X., Ludwig,A., Sautter,A. and Hofmann,F. (1996b) Molecular cloning and expression of a modulatory subunit of the cyclic nucleotide-gated cation channel. *J. Biol. Chem.*, **271**, 6349–6355.

Bönigk,W., Altenhofen,W., Müller,F., Dose,A., Illing,M., Molday,R.S. and Kaupp,U.B. (1993) Rod and cone photoreceptor cells express distinct genes for cGMP-gated channels. *Neuron*, **10**, 865–877.

Bönigk,W., Müller,F., Middendorf,R., Weyand,I. and Kaupp,U.B. (1996) Two alternatively spliced forms of the cGMP-gated channel α-subunit from cone photoreceptor are expressed in the chick pineal gland. *J. Neurosci.*, **16**, 7458–7468.

Bradley,J., Li,J., Davidson,N., Lester,H.A. and Zinn,K. (1994) Heteromeric olfactory cyclic nucleotide-gated channels: a new subunit that confers increased sensitivity to cAMP. *Proc. Natl Acad.. Sci. USA*, **91**, 8890–8894.

Bradley,J., Zhang,Y., Bakin,R., Lester,H.A., Ronnett,G.V. and Zinn,K. (1997) Functional expression of the heteromeric 'olfactory' cyclic nucleotide-gated channel in the hippocampus: a potential effector of synaptic plasticity in brain neurons. *J. Neurosci.*, **17**, 1993–2005.

Burnashev,N., Zhou,Z., Neher,E. and Sakmann,B. (1995) Fractional calcium currents through recombinant GluR channels of the NMDA, AMPA and kainate receptor subtypes. *J. Physiol.*, **485**, 403–418.

Chen,C. and Okayama,H. (1987) High-efficiency transformation of mammalian cells by plasmid DNA. *Mol. Cell. Biol.*, **7**, 2745–2752.

Chen,T.Y., Illing,M., Molday,L.L., Hsu,Y.T., Yau,K.W. and Molday,R.S. (1994) Subunit 2 (or β) of retinal rod cGMP-gated cation channel is a component of the 240-kDa channel-associated protein and mediates Ca^{2+}-calmodulin modulation. *Proc. Natl Acad. Sci. USA*, **91**, 11757–11761.

Coburn,C.M. and Bargmann,C.I. (1996) A putative cyclic nucleotide-gated channel is required for sensory development and function in *C.elegans*. *Neuron*, **17**, 695–706.

Colamartino,G., Menini,A. and Torre,V. (1991) Blockage and permeation of divalent cations through the cyclic GMP-activated channel from tiger salamander retinal rods. *J. Physiol.*, **440**, 189–206.

Corrie,J.E.T. and Trenham,D.R. (1993) Caged cyclic nucleotides and neurotransmitters. In Morrison,H. (ed.), *Bioorganic Photochemistry, Volume 2. Structures, Regulation and Drug Action.* John Wiley & Sons, Chichester, UK, pp. 243–305.

Dang,T.X. and McCleskey,E.W. (1998) Ion channel selectivity through stepwise changes in binding affinity. *J. Gen. Physiol.*, **111**, 185–193.

De Waard,M., Gurnett,C.A. and Campbell,K.P. (1996) Structural and functional diversity of voltage-activated calcium channels. In Narahashi,T. (ed.), *Ion Channels*. Plenum Press, New York, pp. 41–87.

Dhallan,R.S., Yau,K.W., Schrader,K.A. and Reed,R.R. (1990) Primary structure and functional expression of a cyclic nucleotide-activated channel from olfactory neurons. *Nature*, **347**, 184–187.

Distler,M., Biel,M., Flockerzi,V. and Hofmann,F. (1994) Expression of cyclic nucleotide-gated channels in non-sensory tissues and cells. *Neuropharmacology*, **33**, 1275–1282.

Dryer,S.E. and Henderson,D. (1991) A cyclic CMP-activated channel in dissociated cells of the chick pineal gland. *Nature*, **353**, 756–758.

Eismann,E., Müller,F., Heinemann,S.H. and Kaupp,U.B. (1994) A single negative charge within the pore region of a cGMP-gated channel controls rectification, Ca^{2+} blockage and ionic selectivity. *Proc. Natl Acad. Sci. USA*, **91**, 1109–1113.

El-Husseini,A.E.D., Bladen,C. and Vincent,S.R. (1995) Expression of the olfactory cyclic nucleotide gated channel (CNG1) in the rat brain. *NeuroReport*, **6**, 1459–1463.

Ellinor,P.T., Yang,J., Sather,W.A., Zhang,J.F. and Tsien,R.W. (1995) Ca^{2+} channel selectivity at a single locus for high-affinity Ca^{2+} interactions. *Neuron*, **15**, 1121–1132.

Finn,J.T., Grunwald,M.E. and Yau,K.W. (1996) Cyclic nucleotide-gated ion channels: an extended family with diverse functions. *Annu. Rev. Physiol.*, **58**, 395–426.

Finn,J.T., Krautwurst,D., Schroeder,J.E., Chen,T.Y., Reed,R.R. and Yau,K.-Y. (1998) Functional co-assembly among subunits of cyclic-nucleotide-activated, nonselective cation channels and across species from nematode to human. *Biophys. J.*, **74**, 1333–1345.

Frings,S. (1997) Cyclic nucleotide-gated channels and calcium. An intimate relation. In Corbin,J. and Francis,S. (eds), *Signal Transduction in Health and Disease. Advances in Second Messenger and Phosphoprotein Research.* Lippincott-Raven Publishers, Philadelphia, PA, pp. 75–82.

Frings,S., Lynch,J.W. and Lindemann,B. (1992) Properties of cyclic nucleotide-gated channels mediating olfactory transduction. *J. Gen. Physiol.*, **100**, 45–67.

Frings,S., Seifert,R., Godde,M. and Kaupp,U.B. (1995) Profoundly different calcium permeation and blockage determine the specific function of distinct cyclic nucleotide-gated channels. *Neuron*, **15**, 169–179.

Fujita,Y. *et al*. (1993) Primary structure and functional expression of the ω-conotoxin-sensitive N-type calcium channel from rabbit brain. *Neuron*, **10**, 585–598.

Garaschuk,O., Schneggenburger,R., Schirra,C., Tempia,F. and Konnerth,A. (1996) Fractional Ca^{2+} currents through somatic and dendritic glutamate receptor channels of rat hippocampal CA1 pyramidal neurones. *J. Physiol.*, **491**, 757–772.

Grynkiewicz,G., Poenie,M. and Tsien,R.Y. (1985) A new generation of Ca^{2+} indicators with greatly improved fluorescence properties. *J. Biol. Chem.*, **260**, 3440–3450.

Hagen,V., Dzeja,C., Frings,S., Bendig,J., Krause,E. and Kaupp,U.B. (1996) Caged compounds of hydrolysis-resistant analogues of cAMP and cGMP: synthesis and application to cyclic nucleotide-gated channels. *Biochemistry*, **35**, 7762–7771.

Hagen,V., Dzeja,C., Bendig,J., Baeger,I. and Kaupp,U.B. (1998) Novel caged compounds of hydrolysis-resistant 8-Br-cAMP and 8-Br-cGMP: photolabile NPE esters. *J. Photochem. Photobiol. B*, **42**, 71–78.

Hamill,O.P., Marty,A., Neher,E., Sakmann,B. and Sigworth,F.J. (1981) Improved patch-clamp techniques for high-resolution current recording from cells and cell-free membrane patches. *Pflügers Arch.*, **391**, 85–100.

Haynes,L.W. (1995) Permeation of internal and external monovalent cations through catfish cone photoreceptor cGMP-gated channel. *J. Gen. Physiol.*, **106**, 485–505.

Haynes,L.W., Kay,A.R. and Yau,K.-Y. (1986) Single cyclic GMP-activated channel activity in excised patches of rod outer segment membrane. *Nature*, **321**, 66–70.

Hess,P., Lansman,J.B. and Tsien,R.W. (1986) Calcium channel selectivity for divalent and monovalent cations. Voltage and concentration dependence of single channel current in ventricular heart cells. *J. Gen. Physiol.*, **88**, 293–319.

Karpen,J.W., Zimmerman,A.L., Stryer,L. and Baylor,D.A. (1988) Gating kinetics of the cyclic-GMP-activated channel of retinal rods: flash photolysis and voltage-jump studies. *Proc. Natl Acad. Sci. USA*, **85**, 1287–1291.

Kaupp,U.B. (1995) Family of cyclic nucleotide-gated ion channels. *Curr. Opin. Neurobiol.*, **5**, 434–442.

Kaupp,U.B. and Koch,K.W. (1992) Role of cGMP and Ca^{2+} in vertebrate photoreceptor excitation and adaptation. *Annu. Rev. Physiol.* **54**, 153–175.

Kaupp,U.B. *et al*. (1989) Primary structure and functional expression from complementary DNA of the rod photoreceptor cyclic cGMP-gated channel. *Nature*, **342**, 762–766.

Kim,M.S., Morii,T., Sun,L.X., Imoto,K. and Mori.Y. (1993) Structural determinants of ion selectivity in brain calcium channel. *FEBS Lett.*, **318**, 145–148.

Kingston,P.A., Zufall,F. and Barnstable,C.J. (1996) Rat hippocampal neurons express genes for both rod retinal and olfactory cyclic nucleotide-gated channels: novel targets for cAMP/cGMP function. *Proc. Natl Acad. Sci. USA*, **93**, 10440–10445.

Kleene,S.J. (1994) An electrophysiological survey of frog olfactory cilia. *J. Exp. Biol.*, **195**, 307–328.

Kleene,S.J. (1995) Block by external calcium and magnesium of the cyclic nucleotide-activated current in olfactory cilia. *Neuroscience*, **66**, 1001–1008.

Koch,K.W. (1995) Control of photoreceptor proteins by Ca^{2+}. *Cell Calcium*, **18**, 314–321.

Körschen,H.G. *et al*. (1995) A 240 kDa protein represents the complete β-subunit of cyclic nucleotide-gated channel from rod photoreceptors. *Neuron*, **15**, 627–636.

Korenbrot,J.I. (1995) Ca^{2+} flux in retinal rod and cone outer segments: differences in Ca^{2+} selectivity of the cGMP-gated ion channels and Ca^{2+} clearance rates. *Cell Calcium*, **18**, 285–300.

Leinders-Zufall,T., Rosenboom,H., Barnstable,C.J., Shepherd,G.M. and Zufall,F. (1995) A calcium-permeable cGMP-gated cation conductance in hippocampal neurons. *NeuroReport*, **6**, 1761–1765.

Leinders-Zufall,T., Rand,M.N., Shepherd,G.M., Greer,C.A. and Zufall,F. (1997) Calcium entry through cyclic nucleotide-gated channels in individual cilia of olfactory receptor cells: spatiotemporal dynamics. *J. Neurosci.*, **17**, 4136–4148.

Leinders-Zufall,T., Greer,C.A., Shepherd,G.M. and Zufall,F. (1998) Imaging odor-induced calcium transients in single olfactory cilia: specificity of activation and role in transduction. *J. Neurosci.* **18**, 5630–5639.

Li,J., Zagotta,W.N. and Lester,H.A. (1997) Cyclic nucleotide-gated channels: structural basis of ligand efficacy and allosteric modulation. *Q. Rev. Biophys.*, **30**, 177–193.

Liman,E.R. and Buck,L.B. (1994) A second subunit of the olfactory cyclic nucleotide-gated channel confers high sensitivity to cAMP. *Neuron*, **13**, 611–621.

Ludwig,J., Margalit,T., Eismann,E., Lancet,D. and Kaupp,U.B. (1990) Primary structure of cAMP-gated channel from bovine olfactory epithelium. *FEBS Lett.*, **270**, 24–29.

McCleskey,E.W. (1994) Calcium channels: cellular roles and molecular mechanisms. *Curr. Opin. Neurobiol.*, **4**, 304–312.

Menini,A. (1990) Currents carried by monovalent cations through cyclic GMP-activated channels in excised patches from salamander rods. *J. Physiol.*, **424**, 167–185.

Misaka,T., Kusakabe,Y., Emori,Y., Gonoi,T., Arai,S. and Abe,K. (1997) Taste buds have a cyclic nucleotide-gated channel, CNCgust. *J. Biol. Chem.*, **272**, 22623–22629.

Nakatani,K. and Yau,K.W. (1988) Calcium and magnesium fluxes across the plasma membrane of the toad rod outer segment. *J. Physiol.*, **395**, 695–729.

Nawy,S. and Jahr,C.E. (1990) Suppression by glutamate of cGMP-activated conductance in retinal bipolar cells. *Nature*, **346**, 269–271.

Neher,E. and Augustine,G.J. (1992) Calcium gradients and buffers in bovine chromaffin cells. *J. Physiol.*, **450**, 273–301.

Nizzari,M., Sesti,F., Giraudo,M.T., Virginio,C., Cattaneo,A. and Torre,V. (1993) Single-channel properties of cloned cGMP-activated channels from retinal rods. *Proc. R. Soc. Lond. B.*, **254**, 69–74

Park,C.S. and MacKinnon,R. (1995) Divalent cation selectivity in a cyclic nucleotide-gated ion channel. *Biochemistry*, **34**, 13328–13333.

Perry,R.J. and McNaughton,P.A. (1991) Response properties of cones from the retina of the tiger salamander. *J. Physiol.*, **433**, 561–587.

Picones,A. and Korenbrot,J.I. (1995) Permeability and interaction of Ca^{2+} with cGMP-gated ion channels differ in retinal rod and cone photoreceptors. *Biophys. J.*, **69**, 120–127.

Prasher,D.C., Eckenrode,V.K., Ward,W.W., Prendergast F.G. and Cormier,M. (1992) Primary structure of the *Aequorea victoria* green-fluorescent protein. *Gene*, **111**, 229–233.

Reuter,D., Zierold,K., Schröder,W.H. and Frings,S. (1998) A depolarizing chloride current contributes to chemo-electrical transduction in olfactory sensory neurons *in situ*. *J. Neurosci.*, **18**, 6623–6630.

Rieke,F. and Schwartz,E.A. (1994) A cGMP-gated current can control exocytosis at cone synapses. *Neuron*, **13**, 863–873.

Root,M.J. and MacKinnon,R. (1993) Identification of an external divalent cation-binding site in the pore of a cGMP-activated channel. *Neuron*, **11**, 459–466.

Root,M.J. and MacKinnon,R. (1994) Two identical noninteracting sites in an ion channel revealed by proton transfer. *Science*, **265**, 1852–1856.

Sautter,A., Biel,M. and Hofmann,F. (1997) Molecular cloning of cyclic nucleotide-gated channel subunits from rat pineal gland. *Mol. Brain Res.*, **48**, 171–175.

Sautter,A., Zong,X., Hofmann,F. and Biel,M. (1998) An isoform of the rod photoreceptor cyclic nucleotide-gated channel beta subunit expressed in olfactory neurons. *Proc. Natl Acad. Sci. USA*, **95**, 4696–4701.

Savchenko,A., Barnes,S. and Kramer,R.H. (1997) Cyclic-nucleotide-gated channels mediate synaptic feedback by nitric oxide. *Nature*, **390**, 694–698.

Schneggenburger,R. (1996) Simultaneous measurements of Ca^{2+} influx and reversal potentials in recombinant *N*-methyl-D-aspartate receptor channels. *Biophys. J.*, **70**, 2165–2174.

Schneggenburger R., Zhou,Z., Konnerth,A. and Neher,E. (1993) Fractional contribution of calcium to the cation current through glutamate receptor channels. *Neuron*, **11**, 133–143.

Seifert,R., Eismann,E., Ludwig,J., Baumann,A. and Kaupp,U.B. (1999) Molecular determinants of a Ca^{2+}-binding site in the pore of cyclic nucleotide-gated channels: S5/S6 segments control affinity of intrapore glutamates. *EMBO J.*, **18**, 119–130.

Sesti,F., Eismann,E., Kaupp,U.B., Nizarri,M. and Torre,V. (1995) The multi-ion nature of cGMP-gated channel from vertebrate rods. *J. Physiol.*, **487**, 17–36.

Tang,S., Mikala,G., Bahinski,A., Yatani,A., Varadi,G. and Schwartz,A. (1993) Molecular localization of ion selectivity sites within the pore of a human L-type cardiac calcium channel. *J. Biol. Chem.*, **268**, 13026–13029.

Tempia,F., Kano,M., Schneggenburger,R., Schirra,C., Garaschuk,O., Plant,T. and Konnerth,A. (1996) Fractional calcium current through neuronal AMPA-receptor channels with a low calcium permeability. *J. Neurosci.*, **15**, 456–466.

Thompson,S.H. (1997) Cyclic GMP-gated channels in a sympathetic neuron cell line. *J. Gen. Physiol.*, **110**, 155–164.

Trouslard,J., Marsh,S.J. and Brown,D.A. (1993) Calcium entry through nicotinic receptor channels and calcium channels in cultured rat superior cervical ganglion cells. *J. Physiol.*, **468**, 53–71.

Tsien,R.W., Hess,P., McCleskey,E.W. and Rosenberg,R.L. (1987) Calcium channels: mechanism of selectivity, permeation and block. *Annu. Rev. Biophys. Chem.*, **16**, 265–290.

Vernino,S., Rogers,M., Radcliffe,K.A. and Dani,J.A. (1994) Quantitative measurement of calcium flux through muscle and neuronal nicotinic acetylcholine receptors. *J. Neurosci.*, **14**, 5514–5524.

Weyand,I., Godde,M., Frings,S., Weiner,J., Müller,F., Altenhofen,W., Hatt,H. and Kaupp,U.B. (1994) Cloning and functional expression of a cyclic nucleotide-gated channel from mammalian sperm. *Nature*, **368**, 859–863.

Wiesner,B., Weiner,J., Middendorff,R., Hagen,V., Kaupp,U.B. and Weyand,I. (1998) Cyclic nucleotide-gated channels on the flagellum control Ca^{2+} entry into sperm. *J. Cell Biol.*, **142**, 473–484.

Yang,J., Ellinor,P.T., Sather,W.A., Zhang,J.F. and Tsien,R.W. (1993) Molecular determinants of Ca^{2+} selectivity and ion permeation in L-type Ca^{2+} channels. *Nature*, **366**, 158–161.

Yau,K.-Y. and Nakatani,K. (1984) Cation selectivity of light-sensitive conductance in retinal rods. *Nature*, **309**, 352–354.

Zagotta,W.N. and Siegelbaum,S.A. (1996) Structure and function of cyclic nucleotide-gated channels. *Annu. Rev. Neurosci.*, **19**, 235–263.

Zeilhofer,H.U., Kress,M. and Swandulla,D. (1997) Fractional Ca^{2+} currents through capsaicin- and proton-activated ion channels in rat dorsal root ganglion neurones. *J. Physiol.*, **503**, 67–78.

Zhou,Z. and Neher,E. (1993) Calcium permeability of nicotinic acetylcholine receptor channels in bovine adrenal chromaffin cells. *Pflügers Arch.*, **425**, 511–517.

Zimmerman,A.L. and Baylor,D.A. (1986) Cyclic GMP-sensitive conductance of retinal rods consists of aqueous pores. *Nature*, **321**, 70–72.

Zimmerman,A.L. and Baylor,D.A. (1992) Cation interactions within the cyclic GMP-activated channel of retinal rods from tiger salamander. *J. Physiol.*, **449**, 759–783.

Zimmerman,A.L., Karpen,J.W. and Baylor,D.A. (1988) Hindered diffusion in excised membrane patches from retinal rod outer segments. *Biophys. J.*, **54**, 351–355.

Zufall,F. and Firestein,S. (1993) Divalent cations block the cyclic nucleotide-gated channel of olfactory receptor neurons. *J. Neurophysiol.*, **69**, 1758–1768.

Zufall,F., Gordon,M.S. and Barnstable,C.J. (1997) Cyclic nucleotide gated channels as regulators of CNS development and plasticity. *Curr. Opin. Neurobiol.*, **7**, 404–412.

Received September 14, 1998; revised and accepted November 6, 1998